

## **Synthesis and characterization of Locust Bean Gum derivatives and their application in the production of nanoparticles**

Luis Braz<sup>a,b,c,d\*</sup>, Ana Grenha<sup>d,e</sup>, Marta C. Corvo<sup>f</sup>, João Paulo Lourenço<sup>a,g,h</sup>, Domingos  
5 Ferreira<sup>c</sup>, Bruno Sarmiento<sup>ij,k</sup>, Ana M. Rosa da Costa<sup>a\*</sup>

<sup>a</sup>CIQA – Centre of Research in Chemistry of Algarve, Faculty of Sciences and  
Technology, Campus de Gambelas, 8005-139 Faro, Portugal; <sup>b</sup>Centro de Estudos e  
Desenvolvimento em Saúde (CESUAlg), University of Algarve, Avenida Dr. Adelino  
10 da Palma Carlos, 8000-510 Faro, Portugal; <sup>c</sup>Department of Pharmaceutical Technology,  
Faculty of Pharmacy, University of Porto, Rua de Jorge Viterbo Ferreira n.º 228, 4050-  
313 Porto, Portugal; <sup>d</sup>CBMR – Centre for Biomedical Research, University of Algarve,  
Faculty of Sciences and Technology, Campus de Gambelas, 8005-139 Faro, Portugal;  
<sup>e</sup>CCMAR – Centre for Marine Sciences, University of Algarve, Campus de Gambelas,  
15 8005-139 Faro, Portugal; <sup>f</sup>3N|CENIMAT, Department of Materials Science, Faculty of  
Science and Technology, UNL, 2829-516 Caparica, Portugal; <sup>g</sup>Department of Chemistry  
and Pharmacy, Faculty of Science and Technology, University of Algarve, Campus de  
Gambelas, 8005-139 Faro, Portugal; <sup>h</sup>CQE- Centro de Química Estrutural, Instituto  
Superior Técnico, University of Lisbon; <sup>i</sup>3S, Instituto de Investigação e Inovação em  
20 Saúde, Universidade do Porto, Rua Alfredo Allen, 208, 4200-135 Porto, Portugal;  
<sup>j</sup>INEB, Instituto de Engenharia Biomédica, Biocarrier Group, Universidade do Porto,  
Rua Alfredo Allen, 208, 4200-135 Porto, Portugal; <sup>k</sup>Instituto de Investigação e  
Formação Avançada em Ciências e Tecnologias da Saúde, CESPU, Rua Central de  
Gandra, 1317, 4585-116 Gandra, Portugal

\*Corresponding author:

Luis Braz

School of Health - University of Algarve

Avenida Dr. Adelino da Palma Carlos

30 8000-510 Faro, Portugal

Tel.: +351 289800100 – Ext. 7835

Fax: +351 289818419

E-mail address: lvbraz@ualg.pt

35 Ana Maria Rosa da Costa

CIQA – Centre of Research in Chemistry of Algarve

Faculty of Sciences and Technology – University of Algarve

Campus de Gambelas

8005-139 Faro

40 Portugal

Tel.: +351 289 800 100

Fax: +351 289 800 066

E-mail address: amcosta@ualg.pt

45 **Abstract** (150)

The development of LBG-based nanoparticles intending an application in oral immunization is presented. Nanoparticle production occurred by mild polyelectrolyte complexation, requiring the chemical modification of LBG. Three LBG derivatives were synthesized, namely a positively charged ammonium derivative (LBGA) and

50 negatively charged sulfate (LBGS) and carboxylate (LBGC) derivatives. These were characterized by Fourier-transform infrared spectroscopy, elemental analysis, nuclear magnetic resonance spectroscopy, gel permeation chromatography, and x-ray diffraction. As a pharmaceutical application was aimed, a toxicological analysis of the derivatives was performed by both MTT test and LDH release assay.

55 Several nanoparticle formulations were produced using LBGA or chitosan (CS) as positively charged polymers, and LBGC or LBGS as negatively charged counterparts, producing nanoparticles with adequate properties regarding an application in oral immunization.

60 **Highlights** 3 to 5 bullet points (max 85 characters each, including spaces)

- LBG charged derivatives (ammonium, sulfated and carboxylated) were synthesized;
- LBG-based nanoparticles, adequate for drug delivery applications, were produced;
- 65 • Only the LBG ammonium derivative demonstrated severe cytotoxicity in Caco-2 cells;
- Nanoparticles evidenced very mild effect on Caco-2 cell viability.

**Keywords:** Carboxylated locust bean gum; Polyelectrolyte complexation; Polymeric

70 nanoparticles; Sulfated locust bean gum; Tetraalkylammonium locust bean gum

## 1. Introduction

The recent decades have brought to the market many new biomolecules that have been identified as having therapeutic potential. These molecules, which include from proteins

75 and peptides to antigens and nucleic acids, are usually called biopharmaceuticals, meaning that they are biological in nature and manufactured using biotechnology

(Rader, 2008). Although therapeutically promising, biopharmaceuticals are very unstable compounds and their administration is extremely challenging, due to inherent physicochemical and biopharmaceutical properties (Alonso, 2004; Kammona &

80 Kiparissides, 2012). Moreover, the therapeutic action of proteins and protein-based molecules is not only limited by the potential degradation in biological environments, but also compromised by their low ability to reach the therapeutic site of action

(Antosova, Mackova, Kral & Macek, 2009; Casettari & Illum, 2014; Kammona & Kiparissides, 2012). As such, a meaningful challenge for current pharmaceutical

85 scientists has been the need to develop suitable vehicles that permit delivering

macromolecules through alternative routes of administration. Polymeric nanoparticles have been demonstrating to be very promising in oral delivery of biopharmaceuticals, as many works report their effective role in the enhancement of oral drug bioavailability by facilitating cell internalization (Csaba, Garcia-Fuentes & Alonso, 2006; Kadiyala,

90 Loo, Roy, Rice & Leong, 2010). Their reduced size provides an intimate contact with epithelia and, in several occasions, they have shown the capacity to carry the

encapsulated molecules through the epithelium (Csaba, Garcia-Fuentes & Alonso, 2006; de la Fuente, Csaba, Garcia-Fuentes & Alonso, 2008). With respect to oral vaccination,

the design of suitable antigen delivery systems should focus on optimizing antigen  
95 association efficiency, ensuring the maintenance of its stability during association,  
tailoring release kinetics and eliciting high levels of long-lasting antibody and cellular  
immune responses. Nanoparticles may provide extra benefits in oral immunization  
strategies, because Peyer's Patches (PPs) have shown to be a predominant site for  
uptake of particulates (Lavelle & O'Hagan, 2006). Given their role in intestinal  
100 mediated immunization, M cells are the primary targets to consider. A careful selection  
of nanoparticle matrix materials may further help on the potentiation of an immune  
response. In this context, mucoadhesive polymers can contribute to the prolongation on  
the intestinal residence time (Arca, Gunbeyaz & Senel, 2009), potentiating the uptake  
by M cells.

105 Locust bean gum (LBG), also known as carob bean gum, is obtained from the  
endosperm of carob tree (*Ceratonia siliqua*) seeds, where it acts as reserve material. It is  
reported as biocompatible, biosorbable, biodegradable, non-teratogenic and non-  
mutagenic, presenting a mucoadhesive behaviour, and its degradation products are  
excreted readily (Dionísio & Grenha, 2012; Malik, Arora & Singh, 2011a; Pollard et al.,  
110 2007; Sudhakar, Kuotsu & Bandyopadhyay, 2006; Surana, Munday, Cox & Khan,  
1998). Classified by the FDA as a GRAS (Generally Recognized as Safe) material, it is  
approved in most areas of the world for use in the food industry as thickener, stabilizer,  
emulsifier, and gelling agent (E410). It is also used in the pharmaceutical industry as  
excipient in drug formulations, and in biomedical applications (Barak & Mudgil, 2014;  
115 Dionísio & Grenha, 2012; Kawamura, 2008; Prajapati, Jani, Moradiya, Randeria &  
Nagar, 2013). LBG is mainly comprised of high molecular weight (approximately 50  
000 – 3 000 000 Da) neutral galactomannan, consisting in a linear chain of (1-4)-linked  
 $\beta$ -D-mannopyranosyl units with (1-6)-linked  $\alpha$ -D-galactopyranosyl residues as side

chains. The mannose and galactose contents have been reported to be 73-86% and 27-  
120 14%, respectively, which corresponds to a mannose:galactose (M/G) ratio of  
approximately 4:1 (Kawamura, 2008).

Recently, there has been a growing interest in the chemical functionalization of  
polysaccharides, particularly those non-animal derived, mainly by making use of the  
free hydroxyl groups distributed along their backbone, in order to create derivatives  
125 with properties tailored for the desired applications (Mizrahy & Peer, 2012).

In this paper, the chemical modification of LBG, aimed at obtain charged derivatives  
intended for the development of nanoparticulate carriers by polyelectrolyte  
complexation, is described. Two anionic (sulfate - LBGS and carboxylate - LBGC) and  
one cationic (trimethylammonium - LBGA) derivatives were prepared (**Figure 1**). The  
130 former were combined with the positively charged polysaccharide chitosan (CS) and the  
latter with LBGS in order to produce polymeric nanoparticles.

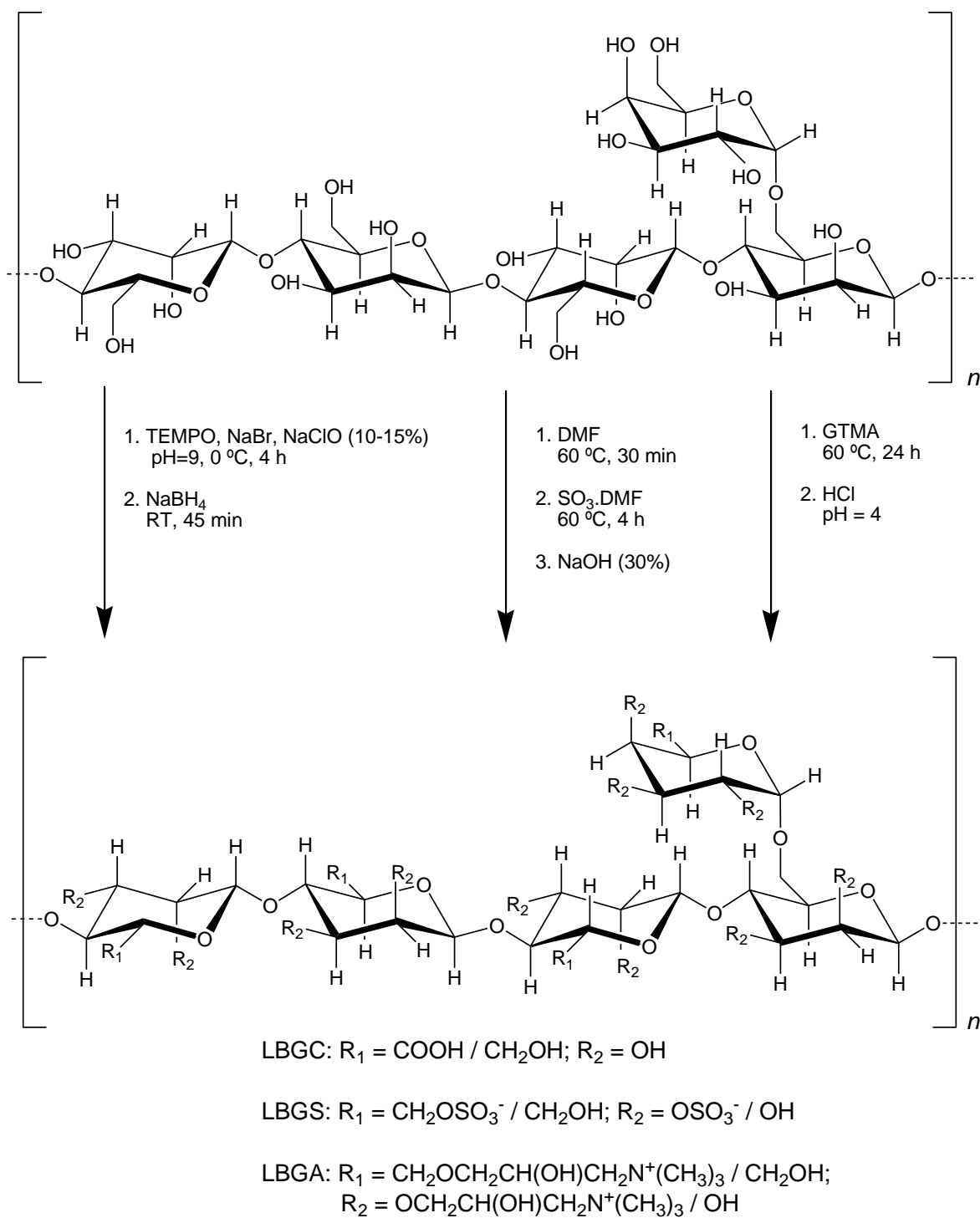


**Figure 1** – Scheme of the chemical modifications introduced in LBG.

## 135 2. Materials and methods

### 2.1. Materials

Locust bean gum (LBG) was a kind gift from Industrial Farensse (Faro, Portugal). Due to the presence of around 3-7% protein in commercial LBG (Kawamura, 2008), a

purification step, based on previously published protocols (Bouzouita et al., 2007; Wang, Wang & Sun, 2002), was performed prior to use. This purified LBG was the material used for subsequent work, unless stated otherwise. Chitosan (CS, low molecular weight, deacetylation degree = 75 – 85%), glacial acetic acid, chlorosulfuric acid (HClSO<sub>3</sub>), dimethylformamide (DMF), *N*-glycidyl-*N,N,N*-trimethylammonium chloride (GTMAC), sodium hydroxide (NaOH), potassium hydroxide (KOH), 2,2,6,6-tetramethylpiperidine-1-oxyl (TEMPO), sodium bromide (NaBr), sodium hypochlorite solution (NaClO), sodium borohydride (NaBH<sub>4</sub>), sodium nitrate (NaNO<sub>3</sub>), sodium dihydrogen phosphate (NaH<sub>2</sub>PO<sub>4</sub>), sodium azide (NaN<sub>3</sub>), dialysis tubing (pore size 2000 Da), phosphotungstate dibasic hydrate, glycerol, phosphate buffered saline (PBS) pH 7.4 tablets, Dulbecco's modified Eagle's medium (DMEM), penicillin/streptomycin (10000 units/mL, 10000 µg/mL), non-essential amino acids, L-glutamine 200 mM, trypsin-EDTA solution (2.5 g/L trypsin, 0.5 g/L EDTA), trypan blue solution (0.4%), thiazolyl blue tetrazolium bromide (MTT), lactate dehydrogenase (LDH) kit, sodium dodecyl sulfate (SDS), dimethyl sulfoxide (DMSO), hydrochloric acid (HCl 37%), sodium chloride (NaCl) and potassium dihydrogen phosphate (KH<sub>2</sub>PO<sub>4</sub>) were purchased from Sigma-Aldrich (Germany). Ethanol was supplied by VWR. Potassium bromide (KBr) was obtained from Riedel-del-Haën (Germany). Fetal bovine serum (FBS) was obtained from Gibco (USA). Ultrapure water (Mili-Q Plus, Milipore Iberica, Madrid, Spain) was used throughout. All other chemicals were reagent grade.

## 160 **2.2. Cell line**

The Caco-2 cell line was obtained from the American Type Culture Collection (Rockville, USA) and used between passages 77-93. Cell cultures were grown in 75 cm<sup>2</sup> flasks in humidified 5% CO<sub>2</sub>/95% atmospheric air incubator at 37 °C. Cell culture



medium was DMEM supplemented with 10% (v/v) FBS, 1% (v/v) L-glutamine  
165 solution, 1% (v/v) non-essential amino acids solution and 1% (v/v)  
penicillin/streptomycin. Medium was changed every 2-3 days and cells were  
subcultured weekly.

## **2.3. Synthesis of Locust Bean Gum derivatives**

### **170 2.3.1. Purification of Locust Bean Gum**

LBG purification was performed as described elsewhere (Braz, Grenha, Ferreira, Rosa  
da Costa, Gamazo & Sarmiento, 2017).

### **2.3.2. Sulfation of Locust Bean Gum**

175 The sulfation agent,  $\text{SO}_3\cdot\text{DMF}$ , was prepared as described before (Braz, Grenha,  
Ferreira, Rosa da Costa, Gamazo & Sarmiento, 2017).

#### *Method 1*

LBG (500 mg) was dispersed in DMF (35 mL) and stirred at 60 °C for 30 min, in order  
180 to provide the dispersion of LBG in the solvent. Then, the  $\text{SO}_3\cdot\text{DMF}$  complex was  
added (9.3 mL) and the mixture reacted for 4 h under magnetic stirring. Subsequently,  
the mixture was cooled down to room temperature in an ice bath, neutralized with 30%  
NaOH solution until precipitation, and concentrated under reduced pressure at 60 °C to  
evaporate the solvent. The residue was dissolved in distilled water (30 mL) and dialyzed  
185 against distilled water (5 L). The water was changed every 24 h and, after 3 days, the  
solution was concentrated under reduced pressure at 40 °C. Then, ethanol was added to  
the concentrated solution, in order to precipitate the solute, and the dispersion was  
concentrated under reduced pressure at 40 °C. The previous step was repeated twice,

and the last evaporation was performed until full evaporation of the solvent. The  
190 obtained powder was dried in a vacuum oven at 40 °C for 3 days, affording 407 mg of  
brownish powder that was grinded and stored until further use.

#### *Method 2*

LBG sulfation by this method was performed as described before (Braz, Grenha,  
195 Ferreira, Rosa da Costa, Gamazo & Sarmiento, 2017).

#### **2.3.3. Carboxylation of Locust Bean Gum**

LBG (500 mg) was dissolved in 200 mL of distilled water under stirring at 80 °C for 30  
min. After cooling down, the volume was adjusted to 200 mL and the solution was  
200 cooled in an ice bath. Then, TEMPO (10 mg) and NaBr (50 mg) were added to the  
solution under stirring. A 15% sodium hypochlorite solution (3.0 mL) with pH adjusted  
to 9.3 with 2 M HCl solution, was mixed with the polymer solution. The pH was  
maintained at 9.3 by addition of a 0.05 M aqueous NaOH solution for 4 h. To stop the  
reaction, sodium borohydride (75 mg) was added and the solution was stirred for 45  
205 min. Then the pH of the mixture was adjusted to 8 by addition of HCl before  
precipitation by 2 volumes of ethanol in presence of NaCl (up to 10 g/L). The polymer  
was isolated by filtration under reduced pressure, washed several times with ethanol,  
filtered and dried in a vacuum oven at 30 °C during 3 days. A white powder (529 mg)  
was obtained, grinded and stored until further use.

210

#### **2.3.4. Quaternary ammonium salt of Locust Bean Gum**

An aqueous solution (10 mL) of KOH (0.550 g), was prepared in a round bottom flask,  
under stirring, at 60 °C. Then, purified LBG (506 mg) and 3.72 mL of GTMAC were

added. After 5 h, an equal amount of GTMAC was added to the mixture, which was  
215 allowed to react until the completion of 24 h. It was then diluted with 20 mL of miliQ  
water, allowed to cool down to room temperature, and neutralized with HCl (2M). The  
resulting solution was dialyzed for 3 days, the water being replaced every 24 h. Then,  
the LBGA solution was concentrated under reduced pressure at 40 °C and ethanol was  
added to the concentrated solution, in order to precipitate the solute. The dispersion was  
220 concentrated under reduced pressure at 40 °C and ethanol was added again and  
evaporated under the same conditions until full evaporation of the solvent. The obtained  
powder was dried in a vacuum oven at 40 °C for 3 days, affording 423 mg of white  
powder that was grinded and stored until further use.

## 225 **2.4. Chemical characterization of Locust Bean Gum derivatives**

### **2.4.1. Fourier transform infrared (FTIR) spectroscopy**

For recording FTIR spectra of purified LBG and their derivatives, samples were  
grounded with KBr in a mortar and compressed into discs. For each spectrum, a 32-scan  
interferogram was collected in transmittance mode with a 4 cm<sup>-1</sup> resolution in the 4,000-  
230 400 cm<sup>-1</sup> region.

### **2.4.2. Elemental analysis**

Elemental analysis data were obtained in a Thermo Finnigan, FLASH EA 1112 Series  
(C, N, S) or in a Fisons Instruments, EA 1108 CHNS-O (O) elemental analyzer.

235

### **2.4.3. Nuclear magnetic resonance (NMR) spectroscopy**

All liquid NMR spectra were acquired in a Bruker Avance III 400 spectrometer  
equipped with a temperature control unit and a pulse gradient unit capable of producing

magnetic field pulsed gradients in the z-direction of 56.0 G/cm, operating at 400.15  
240 MHz for hydrogen, 100.61 MHz for carbon, using a multinuclear reverse 5 mm probe  
(TXI). The samples were dissolved in D<sub>2</sub>O. Solid state NMR spectra were acquired in  
a Bruker Avance III 300 spectrometer equipped with a BBO probehead, operating at  
300.15 MHz for hydrogen, 75.00 MHz for carbon. The sample was spun at the magic  
angle at a frequency of 5 kHz in a 4 mm-diameter rotor at room temperature.

245 <sup>1</sup>H NMR spectra were recorded with 8.22 KHz spectral window digitized with 64 K  
points. The <sup>13</sup>C spectra were recorded between 0 and 238 ppm using 24,000 Hz spectral  
window digitized into 64 K points.

Two-dimensional <sup>1</sup>H-<sup>1</sup>H correlation spectroscopy (**COSY**) spectra were acquired using  
32 transients and 16 dummy scans, with a spectral width of 5000 in a total of 2K data  
250 points in *F2* and 128 data points in *F1*, the relaxation delay was set to 1.5 s.

Heteronuclear Single Quantum Coherence-Total Correlation Spectroscopy (<sup>1</sup>H/<sup>13</sup>C  
**HSQC-TOCSY**) spectra were acquired using the following parameters: 2K data points  
in *F2* with a spectral width of 5000 Hz, 512 data points in *F1* with a spectral width of 17  
KHz, a relaxation delay of 2 s, MLEV-17 sequence with a mixing time of 40 ms, 16  
255 transients and 16 dummy scans. The phase-edited heteronuclear single quantum  
correlation (<sup>1</sup>H/<sup>13</sup>C **HSQC-DEPT**) spectra were acquired in 2K data points in *F2* with a  
spectral width of 5000 Hz, 512 data points in *F1* with a spectral width of 17 KHz, a  
relaxation delay of 2 s, 2 to 8 transients and 16 dummy scans. The Heteronuclear  
Multiple Bond Correlation (<sup>1</sup>H/<sup>13</sup>C **HMBC**) spectra were acquired using the following  
260 parameters: 1K data points in *F2* with a spectral width of 5000 Hz, 256 data points in *F1*  
with a spectral width of 22 KHz, a relaxation delay of 2 s, 24 transients and 16 dummy  
scans.

The  $^{13}\text{C}$  MAS NMR experiments were acquired with proton cross polarization (CPMAS) with a contact time of 1.2 ms, and a recycle delay of 2.0 s.

265

#### **2.4.4. GPC/SEC<sup>3</sup> analysis**

Triple detection Gel Permeation Chromatography (GPC/SEC<sup>3</sup>) analysis was performed in a modular system constituted by a degasser, HPLC pump (K-1001) and RI detector (K-2300) from Knauer, and a viscometer and RALLS from Viscotek (Trisec Dual Detector Model 270), using two PL aquagel-OH mixed 8  $\mu\text{m}$ , 300 x 7.5 mm columns. For purified LBG, LBGC and LBGS the eluent was 0.2 M  $\text{NaNO}_3$ , 0.01M  $\text{NaH}_2\text{PO}_4$ , 0.1% w/v  $\text{NaN}_3$ , pH=7, at 1mL/min; the samples were dissolved in the eluent at 1 mg/mL. For LBGA the eluent was 0.5 M  $\text{NaNO}_3$ , 0.01M  $\text{KH}_2\text{PO}_4$ , 0.1% w/v  $\text{NaN}_3$ , pH=2, at the same rate; the sample was dissolved at 1mg/mL in  $10^{-2}$  M HCl.

275

#### **2.4.5. X-ray diffraction (XRD)**

Powder X-ray diffractograms were recorded on a Panalytical X'Pert Pro diffractometer, operating at 45 kV and 35 mA. The patterns of the pristine and modified samples were recorded in the range 5-45 degrees ( $2\theta$ ) with a step size of 0.0167  $^\circ$  and a time per step of 2 000 seconds, using  $\text{CuK}\alpha$  radiation filtered by Ni and an X'Celerator detector. Prior to the analysis, samples were reduced to a fine powder by grinding in a mortar.

280

### **2.5. Production, characterization and safety evaluation of Locust Bean Gum-based nanoparticles**

285 All nanoparticles were prepared by polyelectrolyte complexation, which consists in the electrostatic interaction between the positive and negative charges of the different polymers (Bhattarai, Gunn & Zhang, 2010).

### **2.5.1. Production of CS/LBGS and CS/LBGC nanoparticles**

290 Several mass ratios of CS/LBGC and CS/LBGS (see **Table 1**) were used to prepare the  
nanoparticles by polyelectrolyte complexation. The stock solution of CS, dissolved in  
1% (w/w) acetic acid, was prepared to reach a final concentration of 1.0 mg/mL, while  
those of LBGC and LBGS, dissolved in ultrapure water, had a final concentration of 2.0  
mg/mL. Nanoparticles were prepared as described before (Braz, Grenha, Ferreira, Rosa  
295 da Costa, Gamazo & Sarmiento, 2017).

### **2.5.2. Production of LBGA/LBGS nanoparticles**

Three mass ratios of LBGA/LBGS (2/1, 1/1 and 1/2) were used to prepare the  
nanoparticles by polyelectrolyte complexation. The stock solutions of LBGA and LBGS  
300 were prepared by dissolving the polymers in ultrapure water, at final concentrations of  
0.5 mg/mL and 1.0 mg/mL, respectively. Nanoparticles were prepared as described  
before (Braz, Grenha, Ferreira, Rosa da Costa, Gamazo & Sarmiento, 2017).

### **2.5.3. Characterization of Locust Bean Gum-based nanoparticles**

#### **2.5.3.1. Size, polydispersion index, $\zeta$ potential and production yield**

305 The size,  $\zeta$  potential, polydispersion index (PDI) and production yield were determined  
as described before (Braz, Grenha, Ferreira, Rosa da Costa, Gamazo & Sarmiento,  
2017).

#### **2.5.3.2. Morphological analysis**

310 The morphological examination of LBGA/LBGS nanoparticles was conducted by  
transmission electron microscopy (TEM; JEM-1011, JEOL, Japan). The samples were

stained with 2% (w/v) phosphotungstic acid and placed on copper grids with carbon films (Ted Pella, USA) for TEM observation.

315

#### **2.5.4. Safety evaluation**

The *in vitro* cell viability and cytotoxicity of bulk LBG, purified LBG and the synthesized derivatives was assessed in Caco-2 cells by the MTT and the LDH release assays, respectively. LBG/LBGS nanoparticles were evaluated using the MTT assay.

320 The assays were performed as described before (Braz, Grenha, Ferreira, Rosa da Costa, Gamazo & Sarmiento, 2017).

#### **2.6. Statistical analyses**

The t-test and the one-way analysis of variance (ANOVA) with the pair wise multiple comparison procedures (Holm-Sidak method) were performed to compare two or multiple groups, respectively. All analyses were run using the SigmaStat statistical program (Version 3.5, SyStat, USA) and differences were considered to be significant at a level of  $P < 0.05$ .

### **3. Results and discussion**

#### **3.1. Synthesis and chemical characterization of Locust Bean Gum derivatives**

The syntheses of the three charged LBG derivatives were made by adapting procedures described in the literature for the modification of other polysaccharides. To perform the sulfation reaction,  $\text{SO}_3\text{-DMF}$  was chosen as sulfating agent (Yuan et al., 2005), as it presents advantages over methods involving the manipulation of either pyridine or sulfur trioxide (Alban, Schauerte & Franz, 2002; Mähner, Lechner & Nordmeier, 2001; Mihai, Mocanu & Carpov, 2001). For the synthesis of the sulfate derivative, two

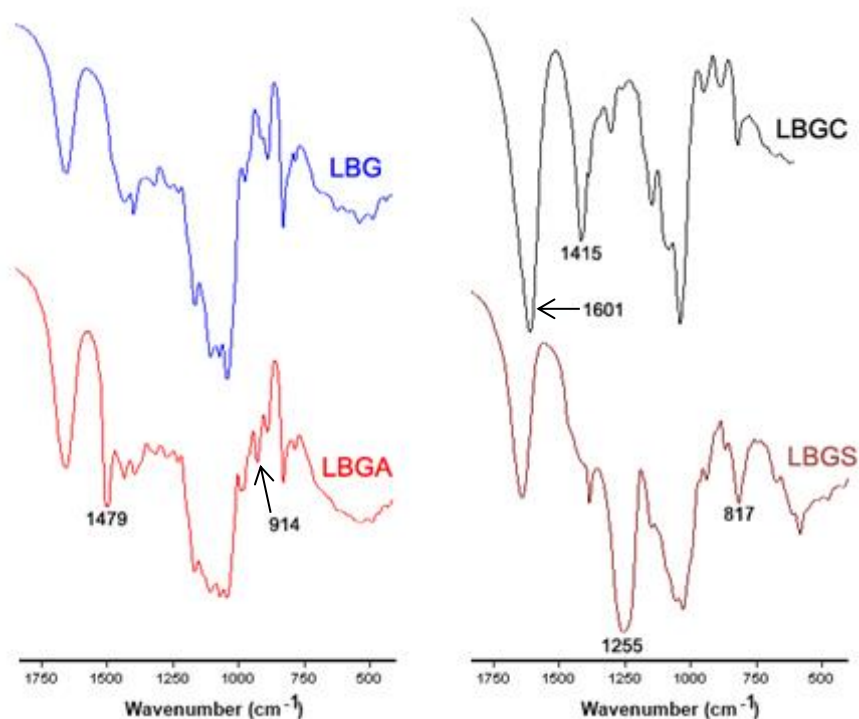
335

approaches were performed as described in the methodology. The difference mainly resided in the processing of LBG prior to the addition of SO<sub>3</sub>-DMF. For the introduction  
340 of trimethylammonium groups in LBG, GTMAC was used as alkylating agent, which proved to be efficient in the alkylation of other polysaccharides (Dionísio, Braz, Corvo, Lourenço, Grenha & da Costa, 2016; Qin et al., 2004; Rekha & Sharma, 2009; Simkovic, Yadav, Zalibera & Hicks, 2009).

For the transformation of LBG into the corresponding polyuronic acid, TEMPO, a  
345 stable nitroxyl radical, was chosen as oxidizing agent (Sierakowski, Milas, Desbrières & Rinaudo, 2000). This has proved to possess a high efficiency in the conversion of high molecular weight polysaccharides. A highly selective oxidation of C-6 primary hydroxyl to carboxylic groups can be achieved in an aqueous solution of the polysaccharide at pH 9-11 with NaClO and catalytic amounts of TEMPO and NaBr  
350 (Cunha, Maciel, Sierakowski, Paula & Feitosa, 2007; da Silva Perez, Montanari & Vignon, 2003; Sierakowski, Milas, Desbrières & Rinaudo, 2000).

As shown in **Figure 2**, LBG sulfate functionalization (LBGS) was confirmed by FTIR, through the appearance of a S=O asymmetric stretching band (Yuan et al., 2005) at 1255 cm<sup>-1</sup> and that of C-O-S symmetric stretching (Alban, Schauerte & Franz, 2002) at  
355 817 cm<sup>-1</sup>. In the carboxylate derivative (LBGC), the absorption bands at 1601 cm<sup>-1</sup> and 1415 cm<sup>-1</sup> are attributed to asymmetric and symmetric stretching vibration of -COO<sup>-</sup>, respectively (Cunha, Maciel, Sierakowski, Paula & Feitosa, 2007). Since the quaternary ammonium groups do not display characteristic IR absorption bands (Nakanishi, Goto & Ohashi, 1957), evidence for formation of the amino functionalized derivative  
360 (LBGA) comes from the broadening of the band at 1088 cm<sup>-1</sup> (ether C-O symmetric stretching) and the new bands at 1479 and 914 cm<sup>-1</sup> (C-H scissoring in methyl groups of the ammonium and ether C-O asymmetric stretching, respectively) (Qin et al., 2004).





365 **Figure 2** – FTIR spectra of purified Locust Bean Gum (LBG) and its ammonium (LBGA), carboxylate (LBGC) and sulfate (LBGS-M1) derivatives.

In the elemental analysis, the weight percentages found for the analysed elements are compiled in **Table S1**.

370 For LBGS, different degrees of substitution were obtained, even under the same reaction conditions. For the sample of LBGS obtained by method 1 (LBGS-M1), a C:S molar ratio of 8.78 was obtained, which corresponds to a degree of substitution (DS) of 3.5. Therefore, if sulfate groups are assumed to be in the form of sodium salts, a molecular formula between  $C_{30}H_{47}S_3O_{34}Na_3$  and  $C_{30}H_{46}S_4O_{37}Na_4$ , to which corresponds

375 a mean molecular weight of 1166 g/mol, is derived. On the other hand, the samples of LBGS obtained by method 2 presented a high variability on C:S molar ratio, ranging from 26.76 in batch 1 (LBGS-M2-B1) to 6.55 in batch 2 (LBGS-M2-B2), and batch 3 (LBGS-M2-B3) presenting a value of 10.24. These values corresponded to values of DS of 1.22, 4.63, and 3, and to the mean molecular weights of 932, 1282, and 1111 g/mol,

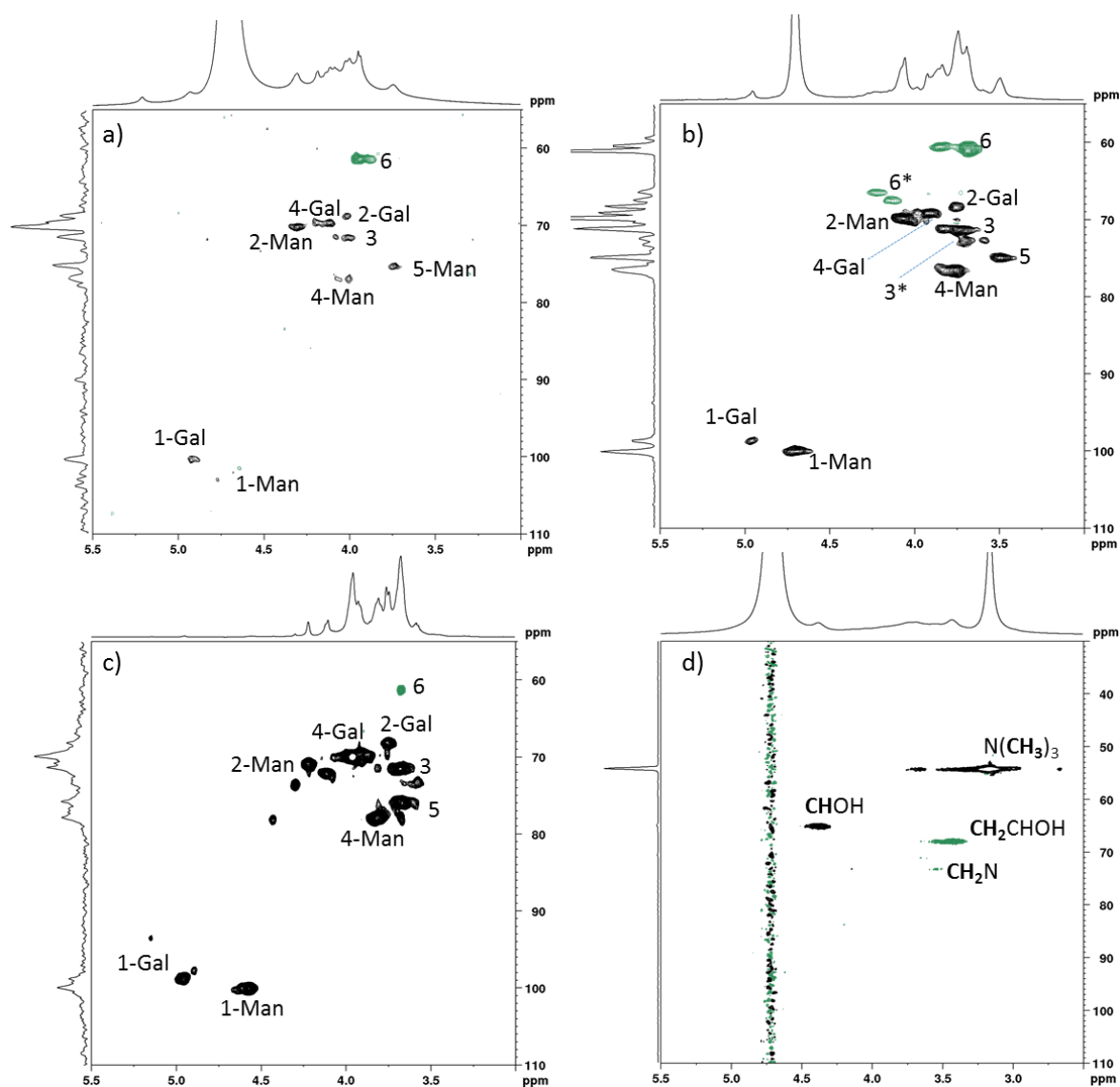
380 respectively. As indicated in materials and methods, and stated above, the difference  
between the two methods only refers to a preliminary treatment of LBG before the  
sulfation reaction. In the second method, a better dispersion of LBG was promoted  
before the contact with the sulfating agent in an attempt to improve the reaction. The  
need for this pre-treatment was motivated by the poor solubility of LBG in DMF. Since  
385 in the sulfation reaction the polymer is used as a dispersion in the solvent, it would be  
expected that a more effective dispersion would favour the reaction. Quite surprisingly,  
it was observed that, although the pre-treatment afforded the highest value of DS (4.63),  
it also gave the lowest substitution (1.22), while in its absence an intermediate value of  
DS was obtained. This variation in DS translates, in the FTIR spectra of the various  
390 samples, in different intensities of the band at  $1255\text{ cm}^{-1}$  relative to other bands in the  
spectrum, with more substituted samples presenting a more intense band (**Figure S1**).  
Assuming that better dispersion of LBG leads to higher reaction efficiency and affords  
higher values of DS, it seems that the dispersibility of LBG in the reaction medium does  
not directly correlate to the method used in its dispersion. One reason for the observed  
395 variability in DS may be the fact that, contrary to what is observed in the reactions  
described below (oxidation and alkylation), in which LBG progressively dissolves as  
the reactions proceed, in this case a total solubilisation is never reached. This renders  
the outcome of this reaction quite unpredictable and, therefore, this issue will have to be  
tackled in future work. In fact, the reaction of LBG activated by pre-soaking in DMF  
400 and dispersed in the same solvent, with solid  $\text{SO}_3\cdot\text{DMF}$  complex, below  $15\text{ }^\circ\text{C}$ , led to a  
DS of approximately 4 (Maiti, Chowdhury, Chakraborty, Ray & Sa, 2014). On the other  
hand, sulfation of LBG dispersed in formamide with  $\text{SO}_3\cdot\text{pyridine}$  complex, under  
diverse conditions of reaction time, temperature, and amount of sulfating agent, led to  
DS varying between approximately 2 and nearly 5 (Wang et al., 2014). Again, the

405 soaking of LBG with the solvent prior to the reaction led to an intermediate DS relative  
to the range obtained without any pre-treatment, although in the latter case a different  
reagent and solvent were used. Nevertheless, only one batch per reaction conditions  
seems to have been obtained in both these works and, therefore, the state of dispersion  
of LBG in each case may well be the factor governing the substitution obtained, instead  
410 of the parameters analysed. Moreover, in the latter work, no correlation or trend  
between molecular weights of the obtained derivatives or depolymerization of the  
parent polysaccharide and degree of substitution is observed. On the contrary, a very  
erratic dispersion of molecular weights with growing DS is obtained, pointing to a  
random behaviour in this reaction.

415 For LBGC, a C:O ratio of 1.02 was found, which corresponds to a degree of oxidation  
(DO) of 4, meaning that all the free C-6 must have been oxidized. Assuming all  
carboxylate groups to be in the sodium salt form, the molecular formula would be  
 $C_{30}H_{38}O_{29}Na_4$ , and the molecular weight 955 g/mol. This value is not surprising, in  
view of the effectiveness of the oxidizing system, although somewhat higher than DO  
420 values observed for other galactomannans, which typically lay below 70% of the free  
units (Cunha, Maciel, Sierakowski, Paula & Feitosa, 2007).

In LBGA, the C:N molar ratio was found to be 13.16, corresponding to a DS of 4.24. If  
all the ammonium groups are in the form of chloride salt, this corresponds to a  
molecular formula between  $C_{54}H_{106}O_{29}N_4Cl_4$  and  $C_{60}H_{120}O_{30}N_5Cl_5$ , and the mean  
425 molecular weight of 1454 g/mol. This corresponds to a full reaction of the free C-6  
hydroxyl groups, along with reaction on some secondary hydroxyls, in line with what  
was observed by us in a similar modification performed in pullulan (Dionísio, Braz,  
Corvo, Lourenço, Grenha & da Costa).

The analysis of the  $^1\text{H}$  NMR and  $^{13}\text{C}$  spectra of LBG and the obtained derivatives  
430 (**Figure S2**) allowed us to obtain a molecular view on the success of the  
transformations. However, the broadened signals in the  $^1\text{H}$  spectra do not allow the  
evaluation of the derivatization locations and, therefore, spectral assignment was  
performed through 2D NMR ( $^1\text{H}$ ,  $^1\text{H}$ -COSY and  $^{13}\text{C}$ ,  $^1\text{H}$ -HSQC-DEPT) experiments.  
**Figure 3** shows the  $^1\text{H}/^{13}\text{C}$  HSQC-DEPT NMR spectra of untreated LBG (**a**), LBGS-  
435 M2-B1 (**b**), LBGC (**c**), and LBGA (**d**). In untreated LBG, the two anomeric carbons C-1  
from mannose and galactose residues resonate at 102.8 and 100.3 ppm, respectively.  
The unsubstituted C-6 positions of main chain mannose exhibited a chemical shift at  
61.4 ppm.



440 **Figure 3** –  $^1\text{H}/^{13}\text{C}$  HSQC-DEPT spectra of (a) LBG, (b) LBGS-M2-B1, (c) LBGC, and  
 445 (d) LBGA; (\*) Assignments attributed to the sulfate derivative.

The attachment of sulfate groups to the hydroxyls results usually in downfield shifts of  
 the carbons bearing the sulfates and the protons linked to them (Duus, Gotfredsen &  
 445 Bock, 2000). LBG primary hydroxyl groups in C-6 position are clearly the most  
 reactive towards the sulfation reaction, as would be expected. In LBGS (**Figure 3-b**),  
 the C-6 resonances exhibit a downfield shift to 66.4 ppm, indicative of C-6 sulfation. It  
 is also noticeable a sulfate introduction in position C-3. The lower steric hindrance in  
 the branched galactose residues in comparison to the main chain mannose leads to the  
 450 assumption that sulfate introduction would have taken place preferentially in the

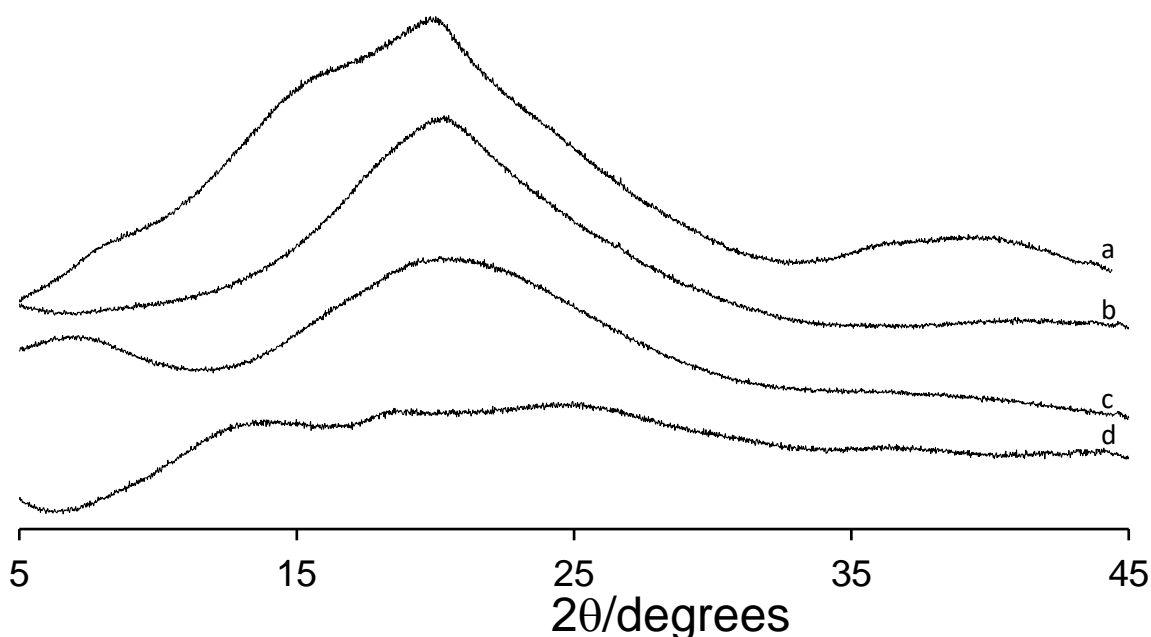
hydroxylated positions of the former, and as such 3-Gal would have been preferentially substituted (Muschin et al., 2016). The carboxylation of LBG imposes a different effect on the  $^1\text{H}/^{13}\text{C}$  HSQC-DEPT spectra, since the resonances of the positions that indeed react are expected to disappear from the original location. From **Figure 3-c** it is possible  
455 to observe that C-6 resonance is almost absent, which means that once again this was the reaction location. Unreacted positions C-2, C-3 and C-4 appear unchanged, while additional resonances appear downshifted from the original envelope of resonances, most likely due to oxidized C-6 positions. The carboxylation is also confirmed by the presence of the carbonyl in the  $^{13}\text{C}$  NMR spectra at 175.3 ppm (**Figure S2-f**). The  
460 attachment of *N*-(2-hydroxypropyl)-*N,N,N*-trimethylammonium to LBG produces a derivative with a high swelling capability. Here, the introduction of the ammonium group is confirmed by the well resolved N-methyl resonances at 3.146 ppm. However, these resonances dominate the whole spectrum (**Figure 3-d**) and all  $^1\text{H}$  signals are very broadened. As such, this sample was analysed in the solid state (**Figure S2-e**), where the  
465 resonances of the ammonium group at 54.62 ppm, the anomeric carbons (102.17 and 100.71 ppm) and the remaining polysaccharide chain between 90 and 60 ppm could be detected.

The average molecular weights, polydispersity index (PDI), and radius of gyration ( $R_g$ ) of LBG and its derivatives are presented in **Table S2**. For the parent polysaccharide  
470 (LBG), these are in general agreement with the literature (Dakia, Blecker, Robert, Whatelet & Paquot, 2008; Kawamura, 2008). Upon chemical modification, an increase in both molecular weight and  $R_g$  was observed in LBGA, and a big decrease in these parameters was patent in LBGC and in the analysed sample of LBGS-M1. The increase identified in LBGA is attributable to the presence of the introduced pendant chains,  
475 which led to an increase in the molar mass of the repeating unit and force the polymer,

once in solution, and similarly to what happens in the crystalline state (XRD results), to adopt a conformation that is suitable to accommodate such bulky groups. The results observed in the LBGC and LBGS-M1 derivatives suggest the occurrence of depolymerization during the chemical modification, a common observation when the conditions of either the oxidation (Cunha, Maciel, Sierakowski, Paula & Feitosa, 2007) or the sulfation reaction (Alban, Schauerte & Franz, 2002) are applied. The latter was already stated in a similar modification performed in pullulan (Dionísio, Braz, Corvo, Lourenço, Grenha & da Costa). Moreover, at least in the analysed sample, and as verified in the referred sulfation of pullulan, no additional dehydration reactions, with intra- and/or intermolecular crosslinking leading to a fraction of high molecular weight chains, observed in sulfation reactions carried out at higher temperatures (Mihai, Mocanu & Carpov, 2001), occurred in this case.

**Figure 4** shows the XRD patterns of the pristine and modified LBG samples. The pattern of LBG, with a broad peak centered at *ca.*  $20^\circ 2\theta$  with shoulders at *ca.*  $7.5$  and  $15^\circ 2\theta$ , reflects the predominantly amorphous nature of the material. These shoulders vanish in the pattern of LBG modified with sulfate (LBGS-M2-B2), probably due to some changes in the organization of the polymer chains imposed by the sulfate groups. In what concerns the ammonium derivative, the pattern clearly shows an increase of intensity for higher d-spacings, which is compatible with an increase of the distance between the polymer chains, due to the long chain bearing the ammonium group (Dionísio, Braz, Corvo, Lourenço, Grenha & da Costa). When compared with the other modifications, the introduction of carboxylate groups gives rise to the highest degree of disruption of the long-range order of the LBG polymer chains. The intensity of the peak that appears at  $20^\circ 2\theta$  in the pattern of the original polymer (LBG) is substantially reduced and new broad peaks are now present at *ca.*  $12$  and  $25^\circ 2\theta$ . This is not

surprising, as the conversion of galactose and mannose units into the corresponding uronic acids would enormously affect the conformation of the polysaccharide chains and, consequently, the way they pack in the solid phase.



505

**Figure 4** – XRD patterns of (a) pristine locust bean gum (LBG), (b) LBGS-M2-B2, (c) LBGA, and (d) LBGC.

### 3.2. Characterization of nanoparticles

510 The production of LBG derivatives described above endowed the polymer with charged groups, enabling the preparation of nanoparticles by polyelectrolyte complexation. This is a mild method occurring in hydrophilic medium, devoid of aggressive conditions such as organic solvents or high shear forces, and involving electrostatic interactions between oppositely charged polymers (Grenha, 2012; Prego, Torres & Alonso, 2005).

515 Three derivatives were synthesized which were used in the production of different formulations of nanoparticles. The negatively charged sulfate and carboxylate derivatives were complexed with chitosan to produce CS/LBGS and CS/LBGC



nanoparticles, respectively. In turn, the ammonium derivative was complexed with the sulfate derivative in the innovative approach of producing LBG-only nanoparticles (LBGA/LBGS). The results regarding the physicochemical characterization of the referred nanoparticle formulations are displayed and discussed below.

### 3.2.1. CS/LBGS and CS/LBGC nanoparticles

The first approach towards the formulation of CS/LBGS and CS/LBGC nanoparticles involved the production of carriers having higher or at least the same amount of LBG derivative comparing to chitosan. In this regard, the starting mass ratios selected for the production of the referred formulations of nanoparticles were 1:1, 1:1.5 and 1:2. In the course of the experiments, the need to test other ratios was identified, not necessarily being coincident for each formulation, thus justifying the slight differences observed between the two formulations.

**Table 1** displays the physicochemical characteristics of CS/LBGS nanoparticles. For the production of these nanoparticles, LBGS corresponding to method 1 was used. With CS/LBGS mass ratios varying between 1:1 and 1:2.5, and recalling that CS amount remains constant in all formulations, it was verified that nanoparticle size generally increased with increasing amounts of LBGS. The minimum size was 364 nm (CS/LBGS = 1:1, w/w) and the highest size was 589 nm (CS/LBGS = 1:2.5, w/w) ( $P < 0.05$ ).

540

**Table 1** - Physicochemical characteristics and production yield of CS/LBGS, CS/LBGC and LBGA/LBGS unloaded nanoparticles (mean  $\pm$  SD;  $n \geq 3$ ). Different letters represent significant differences in each parameter and formulation ( $P < 0.05$ ).

Formulation	Ratio	Size	PdI	Zeta potential	Production
	(w/w)	(nm)		(mV)	yield (%)
CS/LBGS	1:1	364.1 $\pm$ 30.0 <sup>a</sup>	0.34 $\pm$ 0.09	+45.6 $\pm$ 1.2 <sup>d</sup>	37.3 $\pm$ 5.6 <sup>h</sup>
	1:1.25	403.7 $\pm$ 37.7 <sup>ab</sup>	0.40 $\pm$ 0.06	+40.0 $\pm$ 0.8 <sup>e</sup>	58.1 $\pm$ 2.7 <sup>i</sup>
	1:1.5	pp*	1.0 $\pm$ 0.0	-5.9 $\pm$ 4.4 <sup>f</sup>	n.d.
	1:2	500.3 $\pm$ 59.6 <sup>bc</sup>	0.47 $\pm$ 0.08	-23.9 $\pm$ 2.7 <sup>g</sup>	56.6 $\pm$ 7.2 <sup>i</sup>
	1:2.5	589.0 $\pm$ 69.5 <sup>c</sup>	0.54 $\pm$ 0.03	-28.5 $\pm$ 5.0 <sup>g</sup>	n.d.
CS/LBGC	1:0.75	489.9 $\pm$ 63.6 <sup>a</sup>	0.45 $\pm$ 0.04	+45.5 $\pm$ 13.0 <sup>b</sup>	49.0 $\pm$ 5.0 <sup>d</sup>
	1:1	479.1 $\pm$ 30.8 <sup>a</sup>	0.51 $\pm$ 0.07	+42.2 $\pm$ 7.4 <sup>b</sup>	54.3 $\pm$ 7.0 <sup>d</sup>
	1:1.25	828.8 $\pm$ 299.8 <sup>a</sup>	0.64 $\pm$ 0.15	+28.8 $\pm$ 7.3 <sup>b</sup>	n.d.
	1:1.5	pp*	1.0 $\pm$ 0.0	-2.5 $\pm$ 8.3 <sup>c</sup>	n.d.
LBGA/LBGS	1:2	206.6 $\pm$ 5.0 <sup>a</sup>	0.13 $\pm$ 0.03	-27.8 $\pm$ 1.4 <sup>c</sup>	30.0 $\pm$ 8.6 <sup>e</sup>
	1:1	pp	-	-	-
	2:1	368.3 $\pm$ 19.3 <sup>b</sup>	0.38 $\pm$ 0.05	+48.1 $\pm$ 1.5 <sup>d</sup>	16.7 $\pm$ 3.8 <sup>f</sup>

545 n.d.: not determined; pp: precipitate; \*slight precipitation compromised the measurement of this parameter

The registered increase in size as higher amount of LBGS is included in the formulations as compared with CS, might be explained by the increase of total mass of polymers that is present. This effect was also reported in other works using the same  
550 nanoparticle production method (Grenha et al., 2010; Rodrigues, da Costa & Grenha, 2012). Precipitation was found to occur for an intermediate formulation (CS/LBGS = 1:1.5, w/w), being coincident with a zeta potential close to zero (-5.9 mV) that possibly

is not sufficient to provide particle repulsion, thus leading to aggregation. A clear Tyndall effect was observed in all the other nanoparticle formulations. The formulations 1:1 and 1:1.25 (w/w) exhibited a strong positive zeta potential of more than +40 mV. The incorporation of a higher amount of LBGS, from formulation 1:1 to 1:1.25 (w/w) resulted in a corresponding decrease in the zeta potential from +46 mV to +40 mV ( $P < 0.05$ ). The formulations 1:2 and 1:2.5 (w/w) presented a complete shift in the zeta potential as the nanoparticles became negatively charged, with zeta potential reaching -29 mV. Again, the incorporation of a higher amount of LBGS led to a nominal decrease in the zeta potential, although this is not statistically significant. This absolute shift of nanoparticle charge reflects the higher amount of LBGS that is present in the nanoparticles, but also demonstrates that both polymers have different charge density. Zeta potential results are perfectly in line with the charge ratios that were calculated for each formulation of nanoparticles, as is depicted in **Figure 5-a**. This figure shows the effect of charge ratios on the zeta potential of CS/LBGS nanoparticles prepared with varying polymeric ratios.

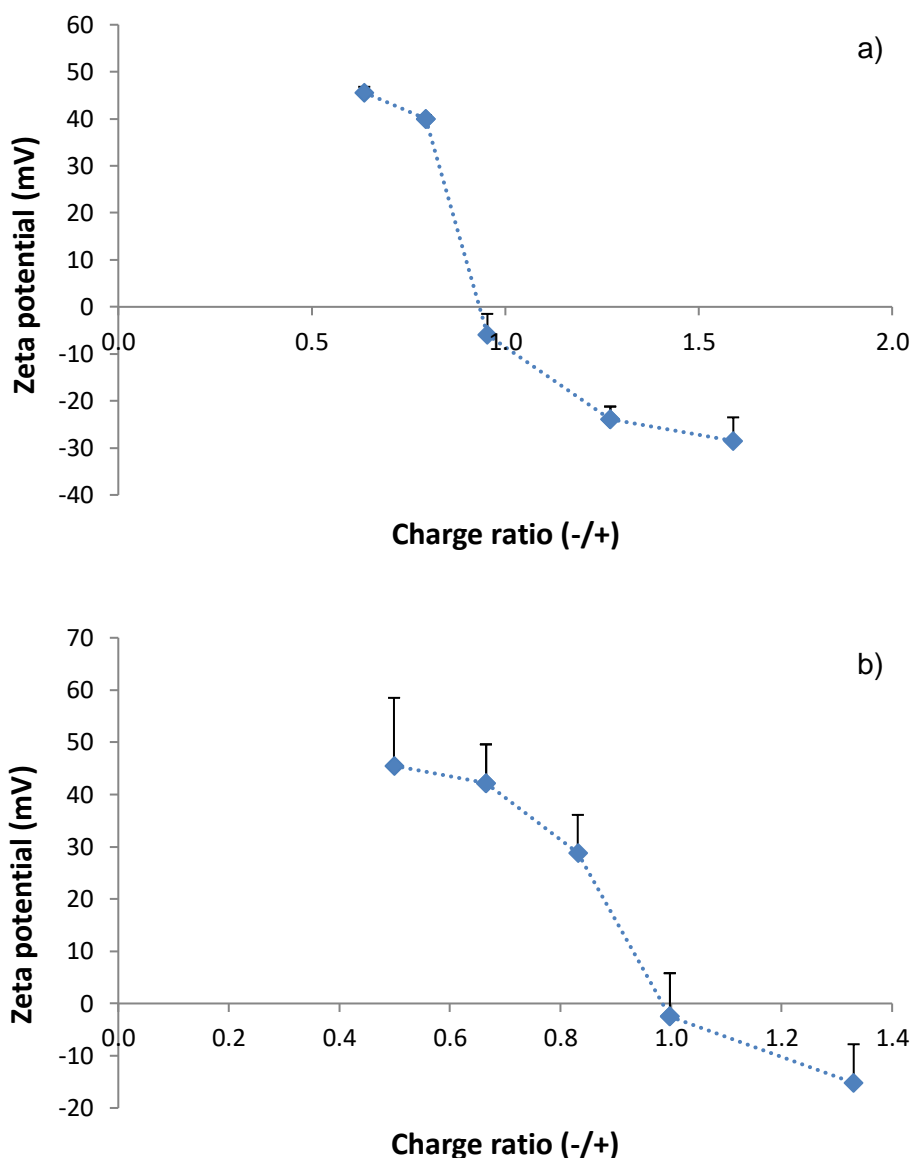


**Figure 5** – Effect of charge ratio (-/+) on the zeta potential of (a) CS/LBGS nanoparticles and (b) CS/LBGC nanoparticles.

570

575 For each polymer, by dividing the charge of the repeating unit by its molar mass, a charge per mass ratio may be obtained. CS has higher charge per mass ratio than LBGS ( $4.72 \times 10^{-3}$  vs  $3.00 \times 10^{-3}$  charges/g, respectively), which justifies why formulations CS/LBGS = 1:1 and 1:1.25 (w/w) have a -/+ charge ratio below 1. The strong positive zeta potential ( $> +40$  mV) of these nanoparticles is due to the predominance of positive

580 charges. In turn, the occurrence of precipitation in the formulation 1:1.5 (w/w) was

coincident with a charge ratio around 1, justifying that the determined zeta potential was close to neutrality. In fact, although a 1:1 +/- charge stoichiometry might not imply the occurrence of complete charge neutralization, due to steric limitations and different charge spacing in the intervenient species (Rodrigues, da Costa & Grenha, 2012), one  
585 may assume a preferential interaction between the sulfate and the ammonium groups, both weakly hydrated, instead of with the strongly hydrated counterions (Crouzier & Picart, 2009). This mainly leads to an intrinsic charge match in detriment of an extrinsic charge compensation and, thus, to a small deviation from neutrality. Finally, the continued addition of the negative polymer (formulations CS/LBGS = 1:2 and 1:2.5,  
590 w/w) produced an excess of negative charges, resulting in +/- charge ratio above 1 and, consequently, negatively charged nanoparticles. A similar behavior concerning the charge ratios leading to either precipitation or formation of nanoparticles, was previously described (Rodrigues, da Costa & Grenha, 2012).

The polydispersity index varied between 0.3 and 0.5, which is considered high.

595 Regarding the production yield, very reasonable values for this nanoparticle production methodology, were obtained. A yield of 37% was registered for formulation 1:1 (w/w) which increased to 58% ( $P < 0.05$ ) for formulation 1:1.25 (w/w). This is a result of the proper mechanism of nanoparticle formation, based on the neutralization of chitosan amino groups by the sulfate groups of LBGS. The incorporation of a higher amount of  
600 LBGS provides an additional amount of sulfate groups that interacted with chitosan, thus forming a higher amount of nanoparticles (Fernández-Urrusuno, Romani, Calvo, Vila-Jato & Alonso, 1999). However, this effect occurs up to a certain limit. As observed, further increasing the amount of LBGS led to precipitation, certainly because of the demonstrated neutralization of charges, as referred above. On keeping increasing

605 LBGS mass, nanoparticles are again formed (CS/LBGS 1:2 and 1:2.5, w/w), this time with an opposite charge and a high yield (57% for formulation 1:2, w/w).

The results obtained for CS/LBGC nanoparticles were rather different comparing to those described above regarding CS/LBGS formulations. In this case, as shown in **Table 1**, the initially approached formulation of CS/LBGC 1:1 (w/w) resulted in a size  
610 of 479 nm, which is more than 30% higher than the corresponding CS/LBGS formulation ( $P < 0.05$ ). The formulation 1:1.5 (w/w) already presented precipitation, similarly to 1:2 (w/w) and, therefore, the intermediate formulation 1:1.25 (w/w) was produced.

The registered size revealed a strong increase to 829 nm, although this is not statistically  
615 significant as is accompanied by an extremely high standard deviation, which indicates reproducibility issues. This formulation also presented a high polydispersity index and, thus, was not characterized for production yield. An attempt was also performed to produce nanoparticles at CS/LBGC ratio of 1:0.75 (w/w), but the characteristics were very similar, under all aspects, to those of ratio 1:1 (w/w). The polydispersity index was  
620 around 0.5 – 0.6, which is even higher than those registered for CS/LBGS nanoparticles, reinforcing the difficulty in producing suitable nanoparticles with the LBGC derivative. The zeta potentials were highly positive (around +45 mV), which probably contributes to the system stability. The determination of the charge ratios involved in each formulation of nanoparticles is depicted in **Figure 5-b**.

625 As observed, formulations 1:0.75 and 1:1 (w/w) have a -/+ charge ratio between 0.5 and 0.7 which does not translate into significant differences in the zeta potential.

Nanoparticles 1:1.25 (w/w) displayed a -/+ charge ratio of 0.85 which induced a nominal decrease of the zeta potential to +29 mV, although not to a statistically significant level. As observed above for CS/LBGS nanoparticles, reaching a -/+ charge

630 ratio around 1 (formulation 1:1.5, w/w) resulted in precipitation. However, in this case  
the continued addition of the negative polymer to formulate CS/LBGC = 1:2 (w/w)  
nanoparticles still resulted in precipitation, despite the -/+ charge ratio of 1.4. It is  
important to highlight that, while the resulting zeta potential for this formulation was of  
-15 mV, in the CS/LBGS corresponding formulation was -24 mV, which possibly  
635 permitted enough repulsion to stabilize the formed nanoparticles.

The determined production yields were satisfactory for this methodology, as referred  
above, being around 50%. When comparing the zeta potentials of these nanoparticles  
with those obtained for CS/LBGS nanoparticles (**Table 1**), a similar trend was  
observed. In this regard, increasing the amount of LBGC present in the formulation  
640 reflected in a decrease of the surface charge, owing to the higher amount of negative  
groups being incorporated. Similarly to CS/LBGS nanoparticles, the formulation 1:1.5  
was the one showing neutrality (zeta potential of -2.5 mV) and the further incorporation  
of LBGC led to a decrease in the surface charge. The precipitation verified for the latter  
was possibly due to the fact that the existing surface charges were not sufficient to  
645 ensure particle repulsion. The resemblance of the trend, particularly regarding the shift  
of the zeta potential (occurring for mass ratio of 1:1.5), suggests the similarity of charge  
density in both derivatives. In fact, LBGS has a charge per mass ratio of  $3.00 \times 10^{-3}$   
charges/g, as stated before, and LBGC has  $3.14 \times 10^{-3}$  charges/g.

### 650 **3.2.2. LBGA/LBGS nanoparticles**

One of the great novelties of producing LBG charged derivatives was the possibility of  
using these to produce, for the first time, LBG-only nanoparticles. Given the difficulties  
in producing nanoparticles with the LBGC derivative, as stated above, it was decided to  
produce the LBG-only nanoparticles using just LBGS as negative counterpart. The

655 nanoparticles were produced by complexation of this derivative (method 2 – 50/50 mixtures of batches 2 and 3) with the ammonium derivative (LBGA) by the same methodology reported in the other cases (polyelectrolyte complexation).

After observing the precipitation of the formulation LBGA/LBGS 1:1 (w/w), possibly resulting from a (-/+) charge ratio of 1.09, formulations 1:2 (w/w) and 2:1 (w/w) were  
660 developed, which results are depicted in **Table 1**.

The formulation containing the highest amount of LBGS registered size of 207 nm and low polydispersity index of 0.13. Naturally, the zeta potential was negative (-28 mV), reflecting the higher content of negatively charged derivative, which translated into a (-/+)  
665 charge ratio of 2.17. As expected, the formulation having more LBGA exhibited a strongly positive zeta potential (+48 mV;  $P < 0.05$ ), as a result of the (-/+) charge ratio of 0.54. However, this particular formulation presented higher size (368 nm) along with higher polydispersity index ( $P < 0.05$ ). At a first evaluation, the size differences could be considered unexpected. In fact, for the preparation of these nanoparticles, LBGA is kept constant at 0.5 mg/mL and LBGS concentration is adapted to meet the desired  
670 ratio. Therefore, formulation 1:2 (w/w) accounts with a total polymeric mass of 1.5 mg, while formulation 2:1 (w/w) accounts with 0.75 mg. In line with this, formulation 1:2 (w/w) was perhaps expected to have larger size. However, if one considers the molecular weight of the derivatives, reported in section 3.3.1, LBGA has much higher  $M_n$  than LBGS (500 600 vs 21 380). In this regard, it becomes justifiable that  
675 nanoparticles having double amount of LBGA comparing with LBGS are those displaying the highest size.

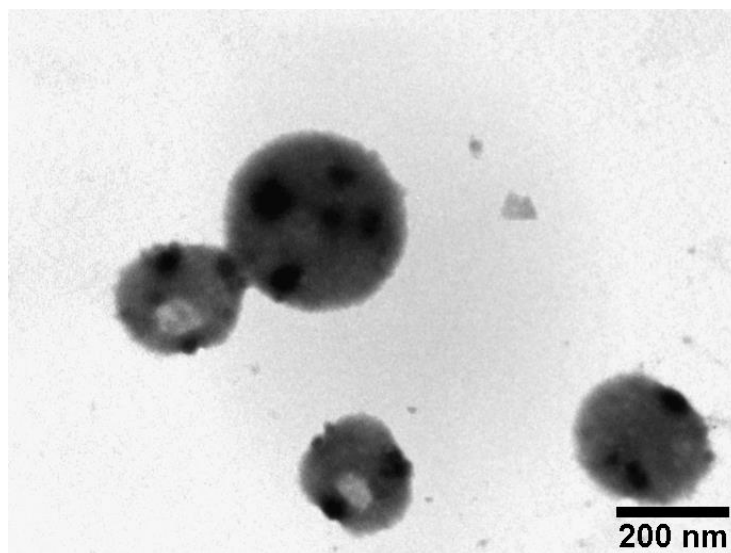
Regarding the production yield, this was very different between the two formulations.

While formulation 1:2 (w/w) resulted in 30%, formulation 2:1 (w/w) presented 17% ( $P < 0.05$ ). This difference is probably due to variances in the molecular weight of the two



680 derivatives. In formulation 1:2 (w/w), there is a determined amount of a high molecular weight polymeric chain and a double amount of a shorter macromolecule that possibly presents higher diffusion. On the contrary, in formulation 2:1 (w/w) the amount of the polymer with higher molecular weight is double comparing with that of the smaller  
685 nanoparticles formed.

LBG-only nanoparticles were morphologically characterized by TEM and the specific formulation LBGA/LBGS 1:2 (w/w) was considered representative for this end. As shown in **Figure 6**, nanoparticles present a spherical shape and have compact structure.

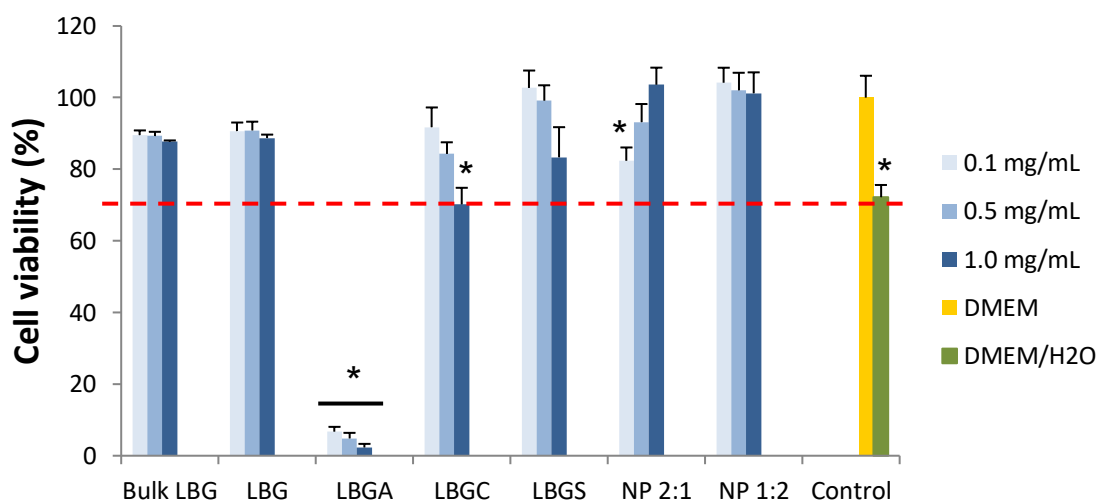


690 **Figure 6** – TEM microphotograph of LBGA/LBGS = 1:2 (w/w) nanoparticles.

### 3.3. Safety evaluation

Caco-2 cells were used to evaluate the toxicological profile of LBG and the synthesized derivatives. Cell viability was determined after exposure to the mentioned materials at  
695 different concentrations, for a period of 3 h (**Figure S3**) and 24 h (**Figure 7**). Cell viability values were calculated in relation to the 100% cell viability considered for the incubation with DMEM (negative control of cell death). The evaluation of LBG-based samples generally evidenced a mild effect on cell viability, considered to be devoid of

biological relevance. In fact, with the exception of LBGA, all the other samples resulted  
 700 in viabilities above 70% after 3 h or 24 h of exposure, when tested at concentrations  
 varying within 0.1 and 1.0 mg/mL. While at 3 h values remained above 88% in all  
 conditions, the prolonged exposure until 24 h induced slight alterations. However, these  
 were in most cases devoid of physiological relevance and the only remarkable effect  
 resides in the decrease of the viability induced by the contact with LBGC at the highest  
 705 concentration tested (1.0 mg/mL) ( $P < 0.05$ ) to a value around 70%. Importantly, this is  
 the value considered by ISO 10993-5 (ISO, 2009) as the level below which a toxic  
 effect is assumed to occur.



710 **Figure 7** – Caco-2 cell viability measured by the MTT assay after 24 h exposure to  
 increasing concentrations of bulk Locust Bean Gum, purified Locust Bean Gum (LBG)  
 and its ammonium (LBGA), carboxylate (LBGC) and sulfate (LBGS) derivatives; and  
 LBGA/LBGS nanoparticles (NP). Data represent mean  $\pm$  SEM ( $n \geq 3$ , six replicates per  
 715 experiment at each concentration). Dashed line indicates 70%. \*  $P < 0.05$  compared  
 with DMEM.

Although not directly proposed herein as matrix material *per se*, unmodified LBG was  
 also tested, because its application in drug delivery has been reported, in many  
 occasions addressing oral delivery strategies (Colombo et al., 1990; Conte & Maggi,  
 720 1996; Coviello, Alhaique, Dorigo, Matricardi & Grassi, 2007; Dey, Sa & Maiti, 2015;

Jana, Gandhi, Sheet & Sen, 2015; Malik, Arora & Singh, 2011a; Malik, Arora & Singh, 2011b; Ngwuluka, Choonara, Kumar, du Toit, Modi & Pillay, 2015; Sandolo, Coviello, Matricardi & Alhaique, 2007; Sujja-areevath, Munday, Cox & Khan, 1998; Syed, Mangamoori & Rao, 2010; Toby, Staniforth, Baichwal & McCall, 1996), but data on  
725 its effect on epithelial cells are not available in the literature. Moreover, a comparison between bulk LBG and purified LBG was performed, revealing no significant differences, which indicates an absence of effect of the purification process in the cytotoxic profile of the material. It is important to mention that the results shown for LBGS sample correspond to the derivative obtained by the second method of synthesis  
730 (method 2 – batch 1), which were similar to those registered for the derivative obtained in the first method (method 1; data not shown).

As mentioned before, LBGA is the material that presents the most distinct behavior, appearing as the exception to the mild effect observed for the tested materials. In fact, a strong decrease of cell viability to approximately 30% was obtained for all the tested  
735 concentrations even upon 3 h exposure (**Figure S3**). The effect was even more drastic after 24 h (**Figure 7**), when a very low level of cell survival was registered ( $P < 0.05$ ). Regarding concentration, there are no evidences of statistically significant concentration-dependent effect. The influence of surface charge on cytotoxicity remains largely unresolved and sometimes the literature reports contradictory results. This is  
740 possibly due to different characteristics of basic materials being used and also to dissimilar assay conditions, which are frequently not described in sufficient detail. Nevertheless, there are many indications suggesting that surface charge has a role on cellular uptake (Fröhlich, 2012; Zhao, Zhao, Liu, Chang, Chen & Zhao, 2011) and on the toxicological effect of substances. In this context, positively charged materials have  
745 been frequently found to be more cytotoxic than neutral or negatively charged

counterparts, because positive charges provide a means for stronger interaction with cell surfaces, in many cases associated with internalization of the material (Bhattacharjee et al., 2010; Fröhlich, 2012; Ilinskaya, Dreyer, Mitkevich, Shaw, Pace & Makarov, 2002; Platel, Carpentier, Becart, Mordacq, Betbeder & Nesslany, 2016; Turcotte, Lavis & Raines, 2009). These statements are coincident with the results of our work, since the neutral (bulk LBG and LBG) and negatively charged materials (LBGC and LBGS) were devoid of toxicity. Another parameter that could be indicated as playing a significant role on toxicity consists on the molecular weight of the polymers. In this regard, although it could be suggested that smaller sizes have higher probability to be internalized by the cells, the literature has been reporting no correlation (Huang, Khor & Lim, 2004). In this work, the molecular weight of the polymers also seems to not be driving the cytotoxic behaviour, as LBGS is the smallest molecule and shows no toxic effect.

Comparing to LBGA, a very similar toxicological profile was observed for an ammonium derivative of another polysaccharide, pullulan, which was synthesized using the same methodology (Dionísio, Braz, Corvo, Lourenço, Grenha & da Costa, 2016; Dionísio, Cordeiro, Remuñán-López, Seijo, Rosa da Costa & Grenha, 2013). In that case, the assessment was performed in Calu-3 cells (bronchial cell line) and cell viabilities around 50-60% were observed after 3 h, decreasing to 40% at 24 h. Although a time-dependent effect is also clearly observed, the effect on cell viability is not as strong as for LBGA. The first consideration to take into account is the fact that the assessment was performed in different cell lines, which may translate into different sensitivity. Additionally, different charge density of the polymers might be indicated as possible justification. In this regard, LBGA has a DS of 4.24, while the corresponding pullulan derivative (ammonium pullulan) has a DS of 2 (Dionísio, Braz, Corvo,

Lourenço, Grenha & da Costa). A higher number of positive charges results in stronger interactions and, thus, in lower cell viability. Complementing this idea, a work reporting the cytotoxic effect of cationic pullulan microparticles on human leukemic K562(S) cells, has established that toxicity increased with the increase molar concentration of amino groups (Constantin, Fundueanu, Cortesi, Esposito & Nastruzzi, 2003). In the work reporting the cytotoxic evaluation of pullulan derivatives, a sulfate derivative of that polysaccharide was also assessed. Similarly to what was observed for LBGS, the registered cell viability was well above 80% (Dionísio, Cordeiro, Remuñán-López, Seijo, Rosa da Costa & Grenha, 2013).

775

780 Considering that polymer samples were solubilized in water and diluted with cell culture medium prior to incubation with the cells, an additional control was performed consisting in a mixture of DMEM and H<sub>2</sub>O in the same ratio used for the samples. This enables a real evaluation of the contribution of the polymers to the final cell viability. The cell viability induced by this control varied between 72% and 80%. Upon 3 h of contact there is a statistically significant difference between the control (DMEM + H<sub>2</sub>O) and all samples, but with LBGS (**Figure S3**). In fact, higher cell viability is observed upon exposure to bulk LBG, LBG and LBGC, suggesting a positive effect of the presence of the polymers. Interestingly, after 24 h exposure, a shift is observed in the effect induced by LBGC and LBGS (**Figure 7**). In the former, the prolonged contact with the cells at the two highest concentrations reverts the positive effect on cell viability observed at 3 h. For LBGS, the results demonstrate that at the two lowest concentrations, the more prolonged contact improves cell viability, which was not registered at 3 h.

785

790

795 One of the most important information provided by the evaluation performed with the MTT assay, is that only the more prolonged exposure to the highest concentration tested

(1.0 mg/mL; 24 h) induced a relevant decrease of Caco-2 cell viability (exception for LBGA). Therefore, it was deemed important to complement the results at these conditions by means of the quantification of the amount of LDH released by Caco-2 cells. To perform this assay, DMEM was used as negative control of LDH release and a lysis buffer was used as positive control. Thus, the negative control (DMEM) corresponds to a normal cell death, while the positive control (lysis buffer) represents 100% cell death.

The results of LDH release after 24 h exposure to the materials at the concentration of 1.0 mg/mL (**Figure S4**) showed no statistically significant differences between the negative control (DMEM), bulk LBG, LBG, LBGC and LBGS. This means that these materials do not compromise Caco-2 cell membrane integrity, as LDH release was not increased when compared with that observed upon incubation with cell culture medium (DMEM). On the contrary, the contact with LBGA resulted in 90% LDH release, which is considered comparable to that induced by the lysis buffer, thus indicating a high cytotoxic effect that results in cell membrane disruption. The results obtained in this assay reinforce those found in the MTT tests, confirming the high cytotoxicity of LBGA.

Overall, the results obtained with these complementary cytotoxicity assays indicate that, with the exception of LBGA, LBG and negatively charged derivatives, present no cytotoxicity towards this *in vitro* intestinal model. This was observed even for the highest concentration tested (1.0 mg/mL) and for prolonged contact (24 h), suggesting their relative safety for an application as matrix materials of oral drug delivery systems. Complementarily, the effect on cell viability provided by LBGS (method 2 – batch 1) was assessed in Calu-3 and A549 cells (respiratory epithelial cells) and the results are in line with those observed for Caco-2 cells (**Figures S5 and S6**).

Proposing materials for drug delivery applications requires testing the developed carriers and not only assume the apparent absence of cytotoxicity of the polymers. In this regard, it is consensual that carriers exhibit new and unique properties, thus generating potential different risks as compared to the raw materials of the same chemistry (Aillon, Xie, El-Gendy, Berkland & Forrest, 2009), as observed in other works (Dionísio, Braz, Corvo, Lourenço, Grenha & da Costa, 2016; Dionísio, Cordeiro, Remuñán-López, Seijo, Rosa da Costa & Grenha, 2013). In this regard, in addition to the evaluation of the polymer and the synthesized derivatives, a preliminary evaluation of LBG-based nanoparticles was further performed using the MTT assay. Although several formulations were proposed and developed herein, that corresponding to LBG-only nanoparticles was selected for this step due to the novelty of the polymer in nanoparticle production.

The viability of Caco-2 cells upon exposure to LBGA/LBGS nanoparticles is shown in **Figure S7** (3 h) and **Figure 7** (24 h). The two formulations LBGA/LBGS 2:1 and 1:2 (w/w) were assessed. For formulation 2:1 (w/w) the comparison of results obtained for each tested time revealed a statistically significant difference between concentrations 0.1 and 1.0 mg/mL ( $P < 0.05$ ). Formulation 1:2 (w/w) did not evidence significant differences between all concentrations at the two tested times. A similar observation was made after comparing the same concentrations for different times (3 h and 24 h). The most remarkable result is that no significant effect on cell viability is observed for both formulations at all concentrations, up to 24 h. Actually, the registered viability was over 80% in all cases, which, as said before, is considered very acceptable according to the ISO10993-5 (ISO, 2009).

Curiously, the exposure of the cells to the formulation LBGA/LBGS 2:1 (w/w) resulted in an increase of cell viability with the increase of nanoparticle concentration at 3 h and

24 h ( $P < 0.05$ ). This was unexpected and may be due to the fact that LBG is a polysaccharide with capacity to promote cell proliferation in some cell lines, as reported in the literature (Perestrelo, Grenha, Rosa da Costa & Belo, 2014). Despite the formulation LBGA/LBGS 2:1 (w/w) could improve cell proliferation with increasing concentrations, formulation LBGA/LBGS 1:2 (w/w), generally induced constant cell viability near 100%, irrespective of the concentration.

Comparing with the control (DMEM + H<sub>2</sub>O) it is observed that the nanoparticles generally elicit higher cell viability, varying between 82% and 100% ( $P < 0.05$ ). The most remarkable observation in the whole set of cell viability assessment is that, in spite of the strong decrease in cell viability induced by the contact with LBGA, this effect was completely reverted when the cells were exposed to a nanoparticulate form of the derivative. This was also observed in works using an ammonium derivative of pullulan, in which the derivative elicited around 40% cell viability upon 24 h of exposure, while nanoparticles produced with the polymer registered increased cell viabilities to values of 70% - 80% (Dionísio, Braz, Corvo, Lourenço, Grenha & da Costa; Dionísio, Cordeiro, Remuñán-López, Seijo, Rosa da Costa & Grenha, 2013). The different impact on cell viability generated by LBGA in form of polymer and of nanoparticles is possibly explained by a differential contact of each of the materials with the cells. While the polymer in form of a solute is presented as an extended chain and, thus, has a higher surface of contact with the cells, nanoparticles have comparatively a lower contact. Additionally, the number of positive charges available for interaction with the negatively charged cells upon complexation with LBGS is significantly decreased, thus decreasing the potential toxicity (Huang, Khor & Lim, 2004). This reinforces the need to evaluate separately the carriers and the raw materials, as the former may exhibit



870 different properties, that may encompass different risks (Aillon, Xie, El-Gendy,  
Berkland & Forrest, 2009).

As also observed for another formulation of LBG-based nanoparticles (CS/LBGS),  
which already shown to be promising for oral immunization (Braz, Grenha, Ferreira,  
Rosa da Costa, Gamazo & Sarmiento, 2017), these preliminary results suggest an  
875 absence of overt toxicity of LBG-only nanoparticles, thus potentiating possible  
applications. Nevertheless, it is recognized that further studies need to be performed to  
reach a more accurate conclusion in this regard.

### **Conclusions**

880 LBG demonstrated to be a good substrate for the production of charged derivatives,  
permitting the synthesis of ammonium, sulfated and carboxylated LBG. Several  
characterization techniques were used to confirm the presence of the new chemical  
groups introduced in each new derivative.

Using a method of polyelectrolyte complexation, the produced derivatives were applied  
885 in the preparation of different formulations of LBG-based nanoparticles, reported herein  
for the first time. When the negatively charged derivatives (sulfated and carboxylated  
LBG) were used, chitosan was the applied positively charged polyelectrolyte. In turn,  
ammonium LBG was complexed with sulfated LBG to obtain LBG-only nanoparticles.  
The physicochemical characteristics of nanoparticles were highly dependent on their  
890 composition and on the charge ratios applied in each complexation being performed.  
Generally, the observed characteristics, with sizes around 200-400 nm in certain cases,  
and tailorable zeta potential according to setup conditions, are suggested as adequate for  
drug delivery applications.

A preliminary toxicological evaluation of LBG derivatives and the produced  
895 nanoparticles was performed, assessing both the metabolic activity and the cell  
membrane integrity of representative intestinal cells (Caco-2) after an exposure of up to  
24 h to concentrations as high as 1 mg/mL. Severe cytotoxicity was found for the  
ammonium derivative of LBG, but this was clearly reverted after the assembly of  
nanoparticles, which evidenced a very mild effect on Caco-2 cell viability. The results  
900 as a whole indicate the possibility to use the synthesized LBG derivatives to produce  
nanoparticles for drug delivery applications.

### **Acknowledgements**

This work was supported by national Portuguese funding through FCT - Fundação para  
905 a Ciência e a Tecnologia, project ref. PTDC/SAU-FCF/100291/2008, PEst-  
OE/EQB/LA0023/2011, UID/QUI/00100/2013, UID/Multi/04326/2013,  
UID/BIM/04773/2013, UID/CTM/50025/2013 and PEst-OE/QUI/UI4023/2014.

This work was also financed by FEDER - Fundo Europeu de Desenvolvimento  
Regional funds through the COMPETE 2020 - Operacional Programme for  
910 Competitiveness and Internationalisation (POCI), Portugal 2020, and by Portuguese  
funds through FCT - Fundação para a Ciência e a Tecnologia/ Ministério da Ciência,  
Tecnologia e Inovação in the framework of the project "Institute for Research and  
Innovation in Health Sciences" (POCI-01-0145-FEDER-007274), POCI-01-0145-  
FEDER-007688 and PTNMR 22161.

915

### **References**

Aillon, K. L., Xie, Y., El-Gendy, N., Berkland, C. J., & Forrest, M. L. (2009). Effects of nanomaterial physicochemical properties on in vivo toxicity. *Advanced Drug Delivery Reviews*, 61(6), 457-466.

- 920 Alban, S., Schauerte, A., & Franz, G. (2002). Anticoagulant sulfated polysaccharides: Part I. Synthesis and structure–activity relationships of new pullulan sulfates. *Carbohydrate Polymers*, 47(3), 267-276.
- Alonso, M. J. (2004). Nanomedicines for overcoming biological barriers. *Biomedicine and Pharmacotherapy*, 58, 168-172.
- 925 Antosova, Z., Mackova, M., Kral, V., & Macek, T. (2009). Therapeutic application of peptides and proteins: parenteral forever? *Trends in Biotechnology*, 27(11), 628-635.
- Arca, H. C., Gunbeyaz, M., & Senel, S. (2009). Chitosan-based systems for the delivery of vaccine antigens. *Expert Reviews of Vaccines*, 8, 937-953.
- Barak, S., & Mudgil, D. (2014). Locust bean gum: Processing, properties and food applications - A review. *International Journal of Biological Macromolecules*, 66, 74-80.
- 930 Bhattacharjee, S., de Haan, L., Evers, N., Jiang, X., Marcelis, A., Zuilhof, H., Rietjens, I., & Alink, G. (2010). Role of surface charge and oxidative stress in cytotoxicity of organic monolayer-coated silicon nanoparticles towards macrophage NR8383 cells. *Particle and Fibre Toxicology*, 7(25), 2-12.
- 935 Bhattarai, N., Gunn, J., & Zhang, M. (2010). Chitosan-based hydrogels for controlled, localized drug delivery. *Adv Drug Deliv Rev*, 62(1), 83-99.
- Bouzouita, N., Khaldi, A., Zgoulli, S., Chebil, L., Chekki, R., Chaabouni, M. M., & Thonart, P. (2007). The analysis of crude and purified locust bean gum: A comparison of samples from different carob tree populations in Tunisia. *Food Chemistry*, 101(4), 1508-1515.
- 940 Braz, L., Grenha, A., Ferreira, D., Rosa da Costa, A. M., Gamazo, C., & Sarmiento, B. (2017). Chitosan/sulfated locust bean gum nanoparticles: In vitro and in vivo evaluation towards an application in oral immunization. *International Journal of Biological Macromolecules*, 96, 786-797.
- Casettari, L., & Illum, L. (2014). Chitosan in nasal delivery systems for therapeutic drugs. *Journal of Controlled Release*, 190, 189-200.
- 945 Colombo, P., Conte, U., Gazzaniga, A., Maggi, L., Sangalli, M. E., Peppas, N. A., & La Manna, A. (1990). Drug release modulation by physical restrictions of matrix swelling. *International Journal of Pharmaceutics*, 63(1), 43-48.
- Constantin, M., Fundueanu, G., Cortesi, R., Esposito, E., & Nastruzzi, C. (2003). Aminated polysaccharide microspheres as DNA delivery systems. *Drug Delivery*, 10(3), 139-149.
- 950 Conte, U., & Maggi, L. (1996). Modulation of the dissolution profiles from Geomatrix® multi-layer matrix tablets containing drugs of different solubility. *Biomaterials*, 17(9), 889-896.
- Coviello, T., Alhaique, F., Dorigo, A., Matricardi, P., & Grassi, M. (2007). Two galactomannans and scleroglucan as matrices for drug delivery: preparation and release studies. *European Journal of Pharmaceutics and Biopharmaceutics*, 66(2), 200-209.
- 955 Crouzier, T., & Picart, C. (2009). Ion pairing and hydration in polyelectrolyte multilayer films containing polysaccharides. *Biomacromolecules*, 10(2), 433-442.
- Csaba, N., Garcia-Fuentes, M., & Alonso, M. J. (2006). The performance of nanocarriers for transmucosal drug delivery. *Expert Opinion on Drug Delivery*, 3(4), 463-478.
- 960 Cunha, P. L. R., Maciel, J. S., Sierakowski, M. R., Paula, R. C. M. d., & Feitosa, J. P. A. (2007). Oxidation of cashew tree gum exudate polysaccharide with TEMPO reagent. *Journal of the Brazilian Chemical Society*, 18, 85-92.
- da Silva Perez, D., Montanari, S., & Vignon, M. R. (2003). TEMPO-mediated oxidation of cellulose III. *Biomacromolecules*, 4(5), 1417-1425.
- 965 Dakia, P., Blecker, C., Robert, C., Whatelet, B., & Paquot, M. (2008). Composition and physicochemical properties of locust bean gum extracted from whole seeds by acid or water dehulling pre-treatment. *Food Hydrocolloids*, 22, 807–818.
- de la Fuente, M., Csaba, N., Garcia-Fuentes, M., & Alonso, M. J. (2008). Nanoparticles as protein and gene carriers to mucosal surfaces. *Nanomedicine*, 3, 845-857.

- 970 Dey, P., Sa, B., & Maiti, S. (2015). Impact of gelation period on modified locust bean-alginate interpenetrating beads for oral glipizide delivery. *International Journal of Biological Macromolecules*, 76, 176-180.
- Dionísio, M., Braz, L., Corvo, M., Lourenço, J. P., Grenha, A., & da Costa, A. M. R. (2016). Charged pullulan derivatives for the development of nanocarriers by polyelectrolyte complexation. *International Journal of Biological Macromolecules*, 86, 129-138.
- 975 Dionísio, M., Cordeiro, C., Remuñán-López, C., Seijo, B., Rosa da Costa, A. M., & Grenha, A. (2013). Pullulan-based nanoparticles as carriers for transmucosal protein delivery. *European Journal of Pharmaceutical Sciences*, 50(1), 102-113.
- Dionísio, M., & Grenha, A. (2012). Locust bean gum: exploring its potential for biopharmaceutical applications. *Journal of Pharmacy and Bioallied Sciences*, 4(3), 75-85.
- 980 Duus, J. Ø., Gotfredsen, C. H., & Bock, K. (2000). Carbohydrate structural determination by NMR spectroscopy: modern methods and limitations. *Chemical Reviews*, 100(12), 4589-4614.
- Fernández-Urrusuno, R., Romani, D., Calvo, P., Vila-Jato, J., & Alonso, M. (1999). Development of a freeze-dried formulation of insulin-loaded chitosan nanoparticles intended for nasal administration. *STP Pharma Sciences*, 9, 429-436.
- 985 Fröhlich, E. (2012). The role of surface charge in cellular uptake and cytotoxicity of medical nanoparticles. *International Journal of Nanomedicine*, 7, 5577-5591.
- Grenha, A. (2012). Chitosan nanoparticles: a survey of preparation methods. *Journal of Drug Targeting*, 20(4), 291-300.
- 990 Grenha, A., Gomes, M. E., Rodrigues, M., Santo, V. E., Mano, J. F., Neves, N. M., & Reis, R. L. (2010). Development of new chitosan/carrageenan nanoparticles for drug delivery applications. *Journal of Biomedical Materials Research Part A*, 92A(4), 1265-1272.
- Huang, M., Khor, E., & Lim, L.-Y. (2004). Uptake and cytotoxicity of chitosan molecules and nanoparticles: Effects of molecular weight and degree of deacetylation. *Pharmaceutical Research*, 21(2), 344-353.
- 995 Ilinkaya, O., Dreyer, F., Mitkevich, V., Shaw, K., Pace, C., & Makarov, A. (2002). Changing the net charge from negative to positive makes ribonuclease Sa cytotoxic. *Protein Science*, 11(10), 2522-2525.
- ISO. (2009). Biological evaluation of medical devices Part 5: Tests for in vitro cytotoxicity. (Vol. 10993-5): International Organization for Standardization.
- 1000 Jana, S., Gandhi, A., Sheet, S., & Sen, K. K. (2015). Metal ion-induced alginate-locust bean gum IPN microspheres for sustained oral delivery of aceclofenac. *International Journal of Biological Macromolecules*, 72, 47-53.
- Kadiyala, I., Loo, Y., Roy, K., Rice, J., & Leong, K. W. (2010). Transport of chitosan-DNA nanoparticles in human intestinal M-cell model versus normal intestinal enterocytes. *European Journal of Pharmaceutical Sciences*, 39, 103-109.
- 1005 Kammona, O., & Kiparissides, C. (2012). Recent advances in nanocarrier-based mucosal delivery of biomolecules. *Journal of Controlled Release*, 161(3), 781-794.
- Kawamura, Y. (2008). Carob Bean Gum Chemical and Technical Assessment. Joint FAO/WHO Expert Committee on Food Additives.
- 1010 Lavelle, E. C., & O'Hagan, D. T. (2006). Delivery systems and adjuvants for oral vaccines. *Expert Opinion on Drug Delivery*, 3, 747-762.
- Mähner, C., Lechner, M. D., & Nordmeier, E. (2001). Synthesis and characterisation of dextran and pullulan sulphate. *Carbohydrate Research*, 331(2), 203-208.
- 1015 Maiti, S., Chowdhury, M., Chakraborty, A., Ray, S., & Sa, B. (2014). Sulfated locust bean gum hydrogel beads for immediate analgesic effect of tramadol hydrochloride. *Journal of Scientific and Industrial Research*, 73, 21-28.
- Malik, K., Arora, G., & Singh, I. (2011a). Locust bean gum as superdisintegrant - Formulation and evaluation of nimesulide orodispersible tablets. *Polimery w Medycynie*, 41(1), 17-28.
- 1020 Malik, K., Arora, G., & Singh, I. (2011b). Taste masked microspheres of ofloxacin: Formulation and evaluation of orodispersible tablets. *Scientia Pharmaceutica*, 79(3), 653-672.

- Mihai, D., Mocanu, G., & Carpov, A. (2001). Chemical reactions on polysaccharides: I. Pullulan sulfation. *European Polymer Journal*, 37(3), 541-546.
- Mizrahy, S., & Peer, D. (2012). Polysaccharides as building blocks for nanotherapeutics. *The Chemistry Society Reviews*, 41, 2623-2640.
- 1025 Muschin, T., Budragchaa, D., Kanamoto, T., Nakashima, H., Ichiyama, K., Yamamoto, N., Shuqin, H., & Yoshida, T. (2016). Chemically sulfated natural galactomannans with specific antiviral and anticoagulant activities. *International Journal of Biological Macromolecules*, 89, 415-420.
- 1030 Nakanishi, K., Goto, T., & Ohashi, M. (1957). Infrared spectra of organic ammonium compounds. *Bulletin of the Chemical Society of Japan*, 30(4), 403-408.
- Ngwuluka, N. C., Choonara, Y. E., Kumar, P., du Toit, L. C., Modi, G., & Pillay, V. (2015). A co-blended locust bean gum and polymethacrylate-NaCMC matrix to achieve zero-order release via hydro-erosive modulation. *AAPS PharmSciTech*, 16(6), 1377-1389.
- 1035 Perestrelo, A. R., Grenha, A., Rosa da Costa, A. M., & Belo, J. A. (2014). Locust bean gum as an alternative polymeric coating for embryonic stem cell culture. *Mater Sci Eng C Mater Biol Appl*, 40, 336-344.
- Platel, A., Carpentier, R., Becart, E., Mordacq, G., Betbeder, D., & Nesslany, F. (2016). Influence of the surface charge of PLGA nanoparticles on their in vitro genotoxicity, cytotoxicity, ROS production and endocytosis. *Journal of Applied Toxicology*, 36(3), 434-444.
- 1040 Pollard, M., Kelly, R., Wahl, C., Fischer, K. P., Windhab, E., Eder, B., & Amadò, R. (2007). Investigation of equilibrium solubility of a carob galactomannan. *Food Hydrocolloids*, 21, 683-692.
- Prajapati, V. D., Jani, G. K., Moradiya, N. G., Randeria, N. P., & Nagar, B. J. (2013). Locust bean gum: A versatile biopolymer. *Carbohydrate Polymers*, 94(2), 814-821.
- 1045 Prego, C., Torres, D., & Alonso, M. J. (2005). The potential of chitosan for the oral administration of peptides. *Expert Opinion on Drug Delivery*, 2, 843-854.
- Qin, C., Xiao, Q., Li, H., Fang, M., Liu, Y., Chen, X., & Li, Q. (2004). Calorimetric studies of the action of chitosan-N-2-hydroxypropyl trimethyl ammonium chloride on the growth of microorganisms. *International Journal of Biological Macromolecules*, 34(1-2), 121-126.
- 1050 Rader, R. A. (2008). (Re)defining biopharmaceutical. *Nature Biotechnology*, 26(7), 743-751.
- Rekha, M. R., & Sharma, C. P. (2009). Blood compatibility and in vitro transfection studies on cationically modified pullulan for liver cell targeted gene delivery. *Biomaterials*, 30(34), 6655-6664.
- 1055 Rodrigues, S., da Costa, A. M., & Grenha, A. (2012). Chitosan/carrageenan nanoparticles: effect of cross-linking with tripolyphosphate and charge ratios. *Carbohydrate Polymers*, 89(1), 282-289.
- Sandolo, C., Coviello, T., Matricardi, P., & Alhaique, F. (2007). Characterization of polysaccharide hydrogels for modified drug delivery. *European Biophysics Journal*, 36(7), 693-700.
- 1060 Sierakowski, M. R., Milas, M., Desbrières, J., & Rinaudo, M. (2000). Specific modifications of galactomannans. *Carbohydrate Polymers*, 42, 51-57.
- Simkovic, I., Yadav, M. P., Zalibera, M., & Hicks, K. B. (2009). Chemical modification of corn fiber with ion-exchanging groups. *Carbohydrate Polymers*, 76, 250-254.
- 1065 Sudhakar, Y., Kuotsu, K., & Bandyopadhyay, A. K. (2006). Buccal bioadhesive drug delivery - A promising option for orally less efficient drugs. *Journal of Controlled Release*, 114, 15-40.
- Sujja-areevath, J., Munday, D. L., Cox, P. J., & Khan, K. A. (1998). Relationship between swelling, erosion and drug release in hydrophilic natural gum mini-matrix formulations. *European Journal of Pharmaceutical Sciences*, 6, 207-217.
- 1070 Surana, S., Munday, D., Cox, P., & Khan, K. (1998). Relationship between swelling, erosion and drug release in hydrophilic natural gum mini-matrix formulations. *European Journal of Pharmaceutical Sciences*, 6, 207-217.

- 1075 Syed, I., Mangamoori, L., & Rao, Y. (2010). Formulation and characterization of matrix and triple-layer matrix tablets for oral controlled drug delivery. *International Journal of Pharmacy and Pharmaceutical Sciences*, 2(3), 137-143.
- Tobyn, M. J., Staniforth, J. N., Baichwal, A. R., & McCall, T. W. (1996). Prediction of physical properties of a novel polysaccharide controlled release system. I. *International Journal of Pharmaceutics*, 128, 113-122.
- 1080 Turcotte, R. F., Lavis, L. D., & Raines, R. T. (2009). Onconase cytotoxicity relies on the distribution of its positive charge. *The FEBS journal*, 276(14), 3846-3857.
- Wang, F., Wang, Y. J., & Sun, Z. (2002). Conformational role of xanthan in its interaction with locust bean gum. *Journal of Food Science*, 67(7), 2609-2614.
- Wang, J., Yang, T., Tian, J., Liu, W., Jing, F., Yao, J., Zhang, J., & Lei, Z. (2014). Optimization of reaction conditions by RSM and structure characterization of sulfated locust bean gum.
- 1085 *Carbohydrate Polymers*, 114, 375-383.
- Yuan, H., Zhang, W., Li, X., Lu, X., Li, N., Gao, X., & Song, J. (2005). Preparation and in vitro antioxidant activity of k-carrageenan oligosaccharides and their oversulfated, acetylated, and phosphorylated derivatives. *Carbohydrate Research*, 340, 685-692.
- 1090 Zhao, F., Zhao, Y., Liu, Y., Chang, X., Chen, C., & Zhao, Y. (2011). Cellular uptake, intracellular trafficking, and cytotoxicity of nanomaterials. *Small*, 7(10), 1322-1337.

## Supplementary material

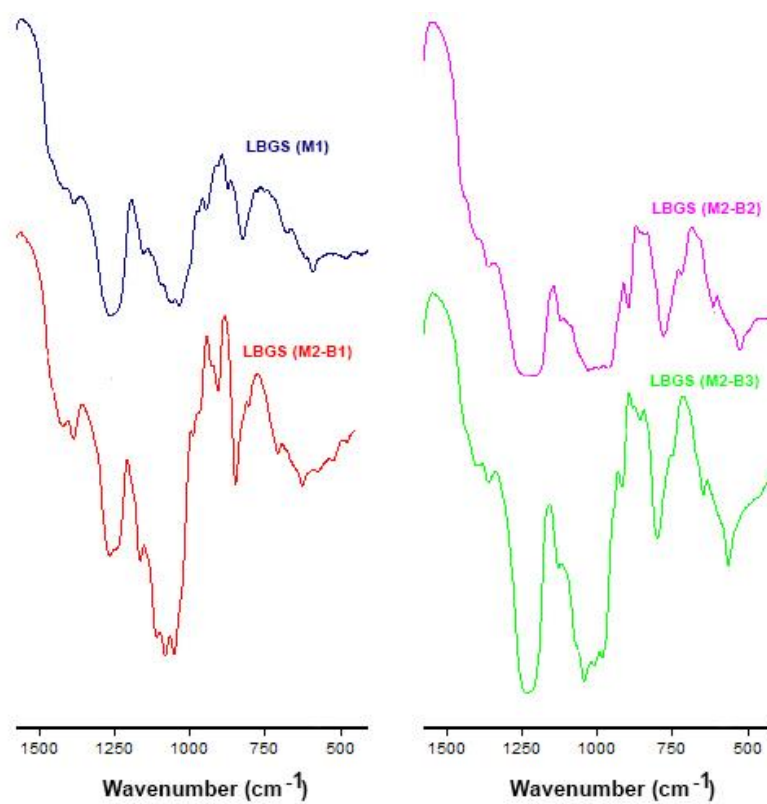


**Figure S1** – FTIR spectra of Locust Bean Gum sulfate derivatives (LBGS) obtained in method 1 (M1) and method 2 (M2). B1, B2 and B3 refer to batch 1, 2 and 3, respectively.

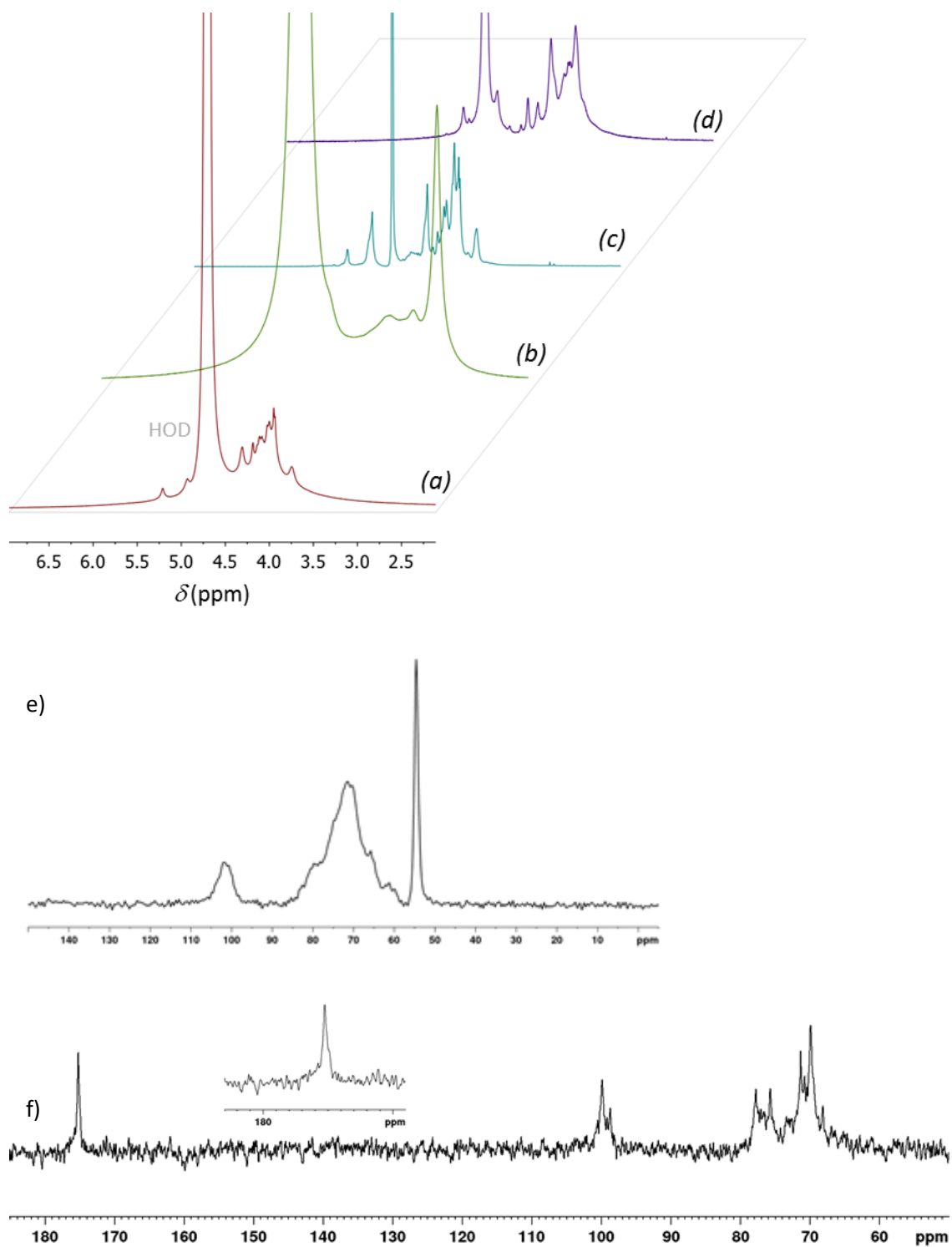


**Figure S2** –  $^1\text{H}$  NMR spectra of (a) LBG, (b) LBGS-M2-B1, (c) LBGC, and (d) LBGA; (e)  $^{13}\text{C}$  CPMAS spectrum of LBGA; (f)  $^{13}\text{C}$  NMR spectrum of LBGC; the big singlet centered at 4.7 ppm in the  $^1\text{H}$  spectra is due to HOD (identified in grey).



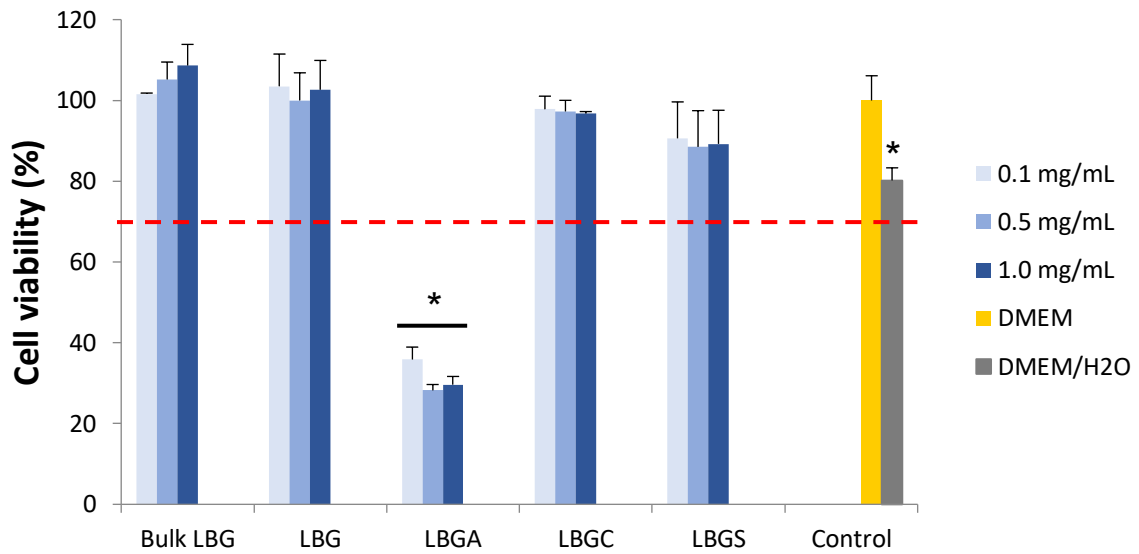


**Figure S3** - Caco-2 cell viability measured by the MTT assay after 3 h exposure to increasing concentrations of bulk Locust Bean Gum, purified Locust Bean Gum (LBG) and its ammonium (LBGA), carboxylate (LBGC) and sulfate (LBGS) derivatives. Data represent mean  $\pm$  SEM ( $n \geq 3$ , six replicates per experiment at each concentration). Dashed line indicates 70%. \*  $P < 0.05$  compared with DMEM.

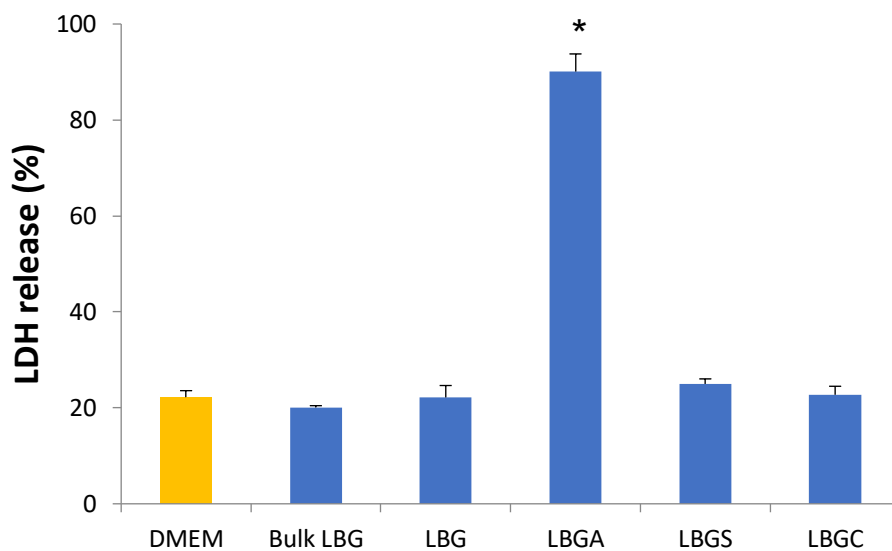


**Figure S4** – Caco-2 cell viability measured by the LDH release assay after 24 h exposure to 1 mg/mL solutions of bulk Locust Bean Gum, purified Locust Bean Gum (LBG) and its ammonium (LBGA), carboxylate (LBGC) and sulfate (LBGS) derivatives. Data represent mean  $\pm$  SEM ( $n \geq 3$ , three replicates per experiment). \*  $P < 0.05$  compared with DMEM.

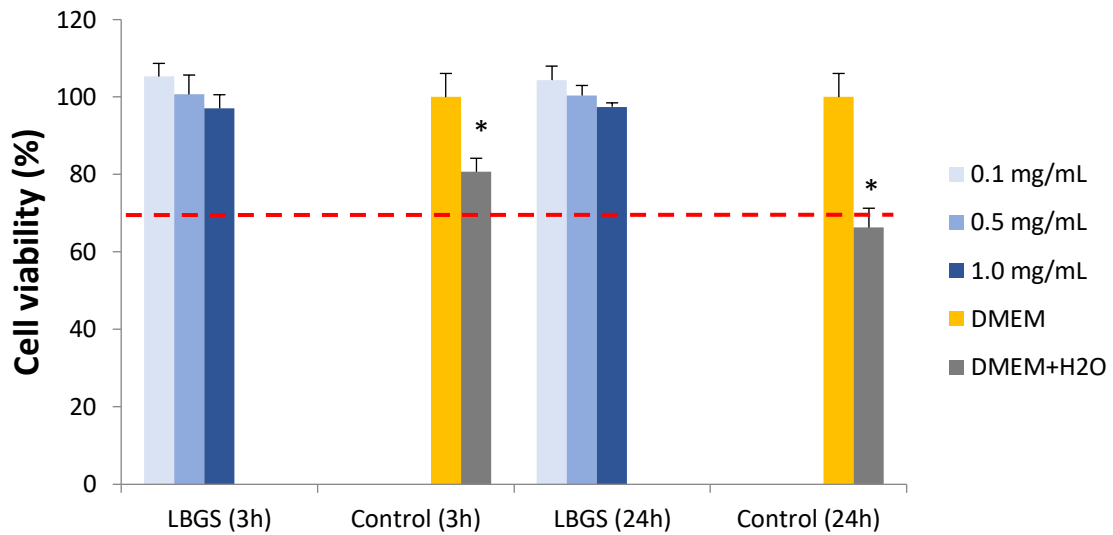


**Figure S5** – A549 cell viability measured by the MTT assay after 3 h and 24 h exposure to increasing concentrations of sulfate locust bean gum (LBGS) derivative. Data represent mean  $\pm$  SEM ( $n \geq 3$ , six replicates per experiment at each concentration). Dashed line indicates 70%. \*  $P < 0.05$  compared with respective control (DMEM).

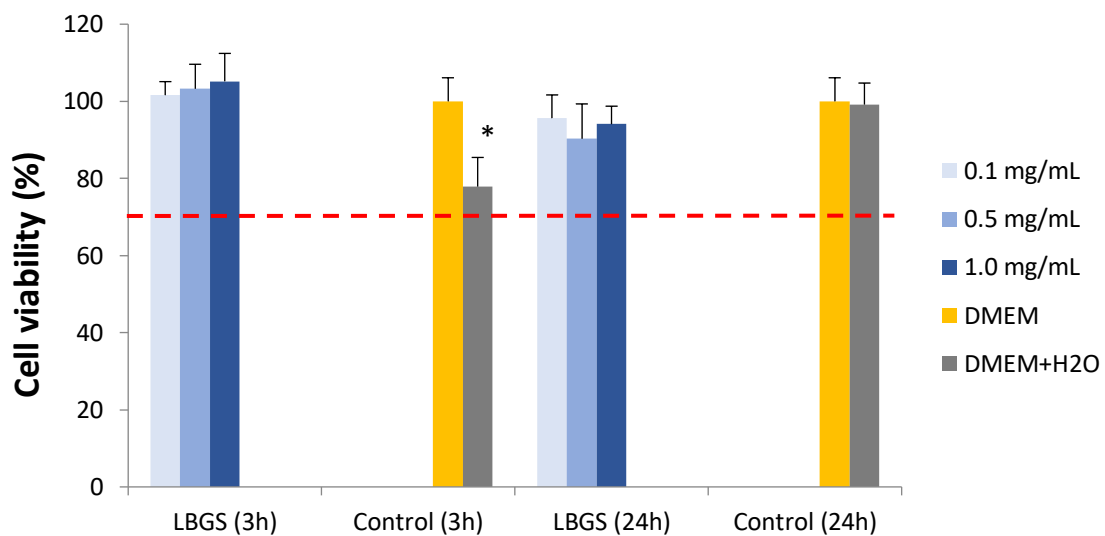


**Figure S6** – Calu-3 cell viability measured by the MTT assay after 3 h and 24 h exposure to increasing concentrations of sulfate locust bean gum (LBGS) derivative. Data represent mean  $\pm$  SEM ( $n \geq 3$ , six replicates per experiment at each concentration). Dashed line indicates 70%. \*  $P < 0.05$  compared with respective control (DMEM).

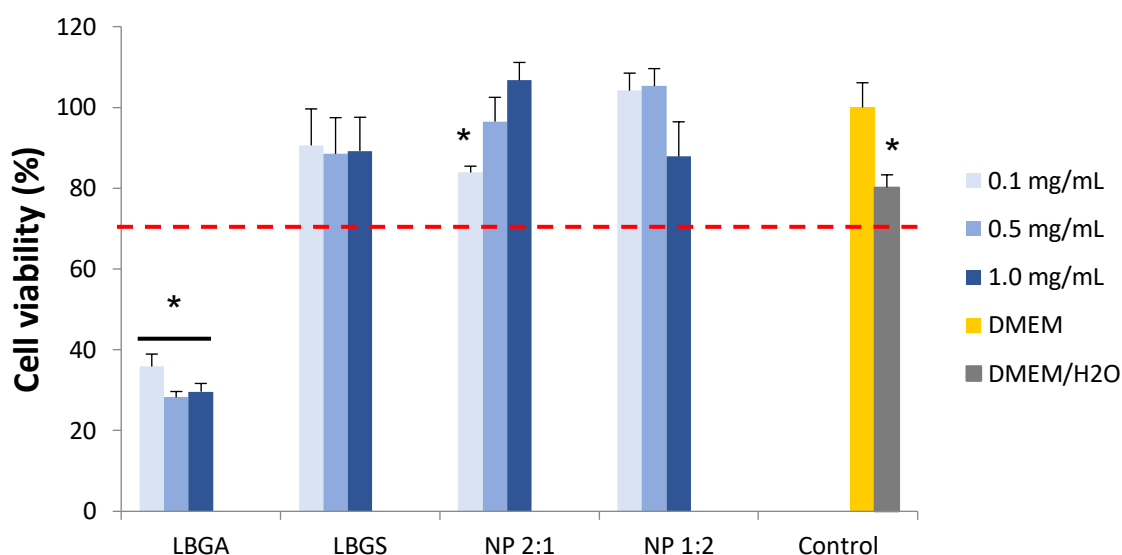


**Figure S7** – Caco-2 cell viability measured by the MTT assay after 3 h exposure to increasing concentrations of ammonium Locust Bean Gum (LBGA) derivative, sulfate Locust Bean Gum (LBGS) derivative and LBGA/LBGS nanoparticles (NP). Data represent mean  $\pm$  SEM ( $n \geq 3$ , six replicates per experiment at each concentration). Dashed line indicates 70%. \*  $P < 0.05$  compared with DMEM.

**Table S1** – Elemental analysis data from the sulfate (LBGS), carboxylate (LBGC) and ammonium (LBGA) derivatives of locust bean gum (LBG).

Element (%)	Polymer					
	LBGS (M1)*	LBGS (M2-B1)*	LBGS (M2-B2)*	LBGS (M2-B3)*	LBGC	LBGA
N	---	---	---	---	---	3.84
C	25.55	35.06	23.94	28.42	37.39	43.39
S	7.77	3.50	9.78	7.41	---	---
O	---	---	---	---	48.96	---

\*B1, B2 and B3 refer to LBGS derivatives from batches 1, 2 and 3, respectively; M1 and M2 refer to LBGS derivatives synthesized with methods 1 and 2, respectively

**Table S2** – GPC analysis of purified Locust Bean Gum (LBG), and its ammonium (LBGA), carboxylate (LBGC) and sulfate (LBGS-M1) derivatives.

<b>Polymer</b>	<b><math>M_n</math> (Da)</b>	<b><math>M_w</math> (Da)</b>	<b>Pdl</b>	<b><math>R_g</math> (nm)</b>
<b>LBG</b>	327 300	589 100	1.80	71.61
<b>LBGA</b>	500 600	871 000	1.74	86.05
<b>LBGC</b>	73 790	119 500	1.62	28.19
<b>LBGS-M1</b>	21 380	26 510	1.24	14.21

$M_n$ : number average molecular weight;  $M_w$ : weight average molecular weight; Pdl: polydispersity index;  $R_g$ : radius of gyration